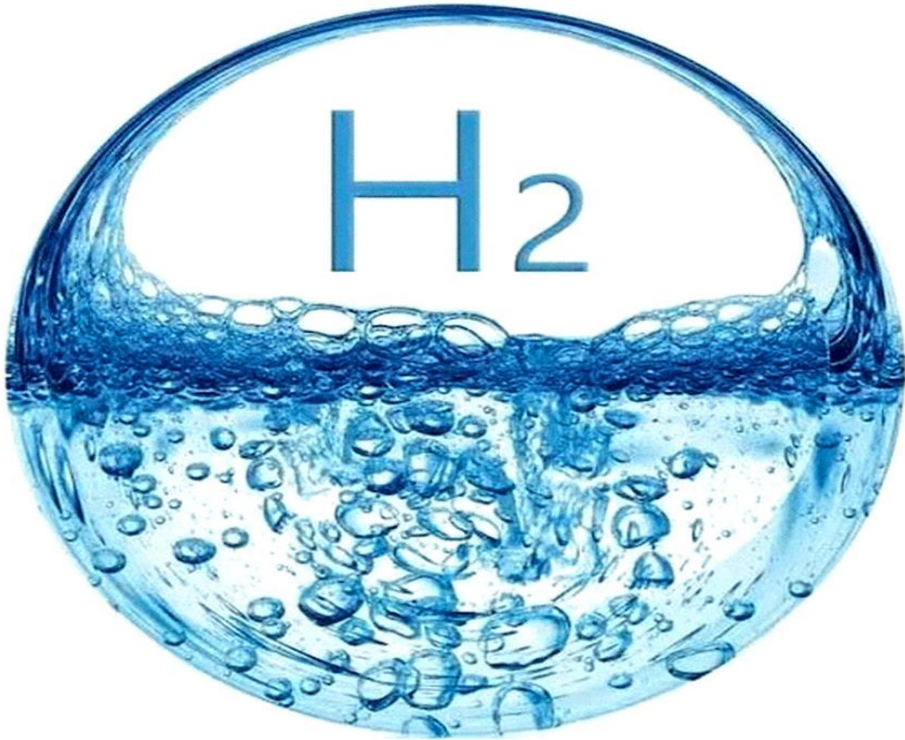


Offshore Solar to Hydrogen

A techno-economic analysis



Christos Zervas

TU Delft

OFFSHORE SOLAR TO HYDROGEN SYSTEM, LOCATED NORTH OF CRETE, GREECE

A TECHNO-ECONOMIC ASSESSMENT

OFFSHORE SOLAR TO HYDROGEN SYSTEM, LOCATED NORTH OF CRETE, GREECE

A TECHNO-ECONOMIC ASSESSMENT

by

Christos Zervas

Student number: 5016797
Project duration: December 2020-September 2021
Faculty: Electrical Engineering, Mathematics & Computer Science
Thesis committee: Prof. dr. A. J. M. van Wijk (Supervisor)
Dr.-Ing. S. Schreier (Supervisor)
Prof. dr. ir. A. H. M. Smets

ACKNOWLEDGEMENTS

At first, I would like to thank my supervisor Prof. dr. Ad van Wijk for his guidance during this Master's thesis. I would like to thank him for giving me the opportunity to work on such an interesting topic and for providing me his great knowledge and experience on the very promising subject of hydrogen.

I would like to also express special gratitude to Dr.-Ing. Sebastian Schreier for being my direct supervisor during this Master's thesis. I would also like to thank him for his guidance and approach through this journey. Not only he helped me face all the challenges that came through, but he also taught me how to manage such a project and work methodically step by step.

I would also like to thank Børge Bjørneklett, the CEO of Ocean Sun, for his cooperation and help on the cost estimates of the floating platform.

Finally, I would like to thank my family for their love and support. Without them, nothing would be possible.

SUMMARY

The energy transition, is one of the most important topics nowadays. Renewable energy sources contribution in the energy mix is growing rapidly. However, due to their intermittent power output, they cannot ensure system security and stability, and therefore, energy storage technologies are needed. In this direction, hydrogen is an energy carrier with great potential. When produced from water electrolysis based on electricity from renewable energy sources (green hydrogen), it represents a sustainable fuel. Due to that, industry's interest is turn on green hydrogen production, with several large scale projects announced on a daily basis. In many countries, especially in Europe, there is not enough empty land for large scale renewable energy projects, turning the interest to offshore areas. This research aims to design and analyse the economic feasibility of an offshore hydrogen production system, intending for 2030, based on offshore solar energy, located in Greece, for the production of a million tons of hydrogen per year. The produced hydrogen will be injected into the European hydrogen network. Considering the main components of an offshore solar to hydrogen system, four possible system configurations are proposed based on two parameters for comparison. The first parameter for examination is the electrolyzer type, which can be either alkaline or PEM. The second parameter is the involvement of batteries into the system. The sizing and cost details about the different systems were selected and all the configurations were modelled using Matlab and Simulink software. From the model results, the levelized cost of hydrogen for all the systems was calculated to evaluate the project. The most cost-effective configuration was the one based on alkaline electrolyzer and without the involvement of batteries. The levelized cost of hydrogen for the selected configuration was calculated to be 1.5 €/kg of hydrogen, making it comparable with blue hydrogen costs and with green hydrogen costs of relevant announced projects. A sensitivity analysis showed that the most influencing factor in the cost calculation is the capital expenditure of the floating photovoltaic system. More specifically, by decreasing the floating photovoltaic costs by 30%, the levelized cost of hydrogen can be reduced by 19%. Finally, in an optimistic scenario, where all influencing factors are improved by 20%, hydrogen can be produced at a cost slightly higher than 1 €/kg. Overall, it is concluded that an offshore hydrogen production system based on offshore floating solar energy, located in Greece, northern to Crete, can produce hydrogen at a competitive cost.

CONTENTS

Acknowledgements	v
Summary	vii
List of Figures	xi
List of Tables	xiii
1 Introduction	1
1.1 Motivation	1
1.2 Aim and research questions	3
1.2.1 Sub-Questions	3
1.3 System Overview	4
1.3.1 Location Survey	4
1.3.2 System Layout	6
1.4 Report Structure	7
2 Literature Review	9
2.1 Hydrogen	9
2.1.1 Hydrogen Project Pipeline	9
2.1.2 Water Electrolysis	10
2.1.3 Reverse Osmosis	15
2.1.4 Hydrogen Storage & Transport	16
2.2 Solar Energy	17
2.2.1 Photovoltaic Basics	17
2.2.2 Floating Photovoltaic Systems	18
2.2.3 FPV System Components	21
2.3 Batteries	24
2.4 Floating Platforms	25
3 System Design	27
3.1 Floating PV	27
3.1.1 PV Modules	27
3.1.2 Balance of System	28
3.2 Electrolyser system	29
3.3 Other Components	31
3.3.1 Battery	31
3.3.2 Compressor	32

4	System Modeling	33
4.1	Overview of system configurations	33
4.1.1	Configurations without batteries.	34
4.1.2	Configurations with batteries	36
4.2	Component Modelling	40
4.2.1	FPV System	40
4.2.2	Electrolyzer Model.	41
4.2.3	Batteries	42
4.2.4	Compressor Model.	43
4.2.5	Pipelines	44
4.2.6	Levelized Cost of Hydrogen	45
5	Results	47
5.1	Configuration Comparison	47
5.2	Final System Overview	48
5.2.1	Sizing Results	48
5.2.2	Artist's Impression	49
5.2.3	Cost Drivers	51
5.3	Sensitivity Analysis	51
5.3.1	Assumptions.	51
5.3.2	Sensitivity	53
5.4	Scenario Analysis	54
6	Discussion	57
7	Conclusion & Recommendations	61
7.1	Conclusion	61
7.2	Future Research Recommendations	64
	Bibliography	65
A	Appendix	75
B	Appendix	79
B.1	Model Results.	79
B.1.1	Configurations without Batteries.	79
B.1.2	Configurations with Batteries	83

LIST OF FIGURES

1.1	Hydrogen production and consumption in 2019 [6]	2
1.2	Global average solar irradiance [12]	3
1.3	Selected location for the power to hydrogen system examined	4
1.4	Depth variation along with the distance from shore for the selected location [13]	5
1.5	Mean Significant Wave Height (SWH), standard deviation of SWH, maximum SWH in meters, respectively [15]	5
1.6	Irradiance data for a typical meteorological year [16]	5
1.7	Irradiance data for a single week of the year [16]	6
1.8	Overview of the system configuration	7
2.1	Hydrogen projects worldwide [21]	9
2.2	Basic electrolytic cell for water electrolysis [24]	11
2.3	Operating principle of alkaline water electrolysis [22]	12
2.4	Operating principle of PEM water electrolysis [22]	14
2.5	LCOE for different renewable energy sources (2019 data) [47]	17
2.6	Characteristic I-V curve of a PV module [49]	18
2.7	Floating PV plants	19
2.8	Global installed FPV capacity and annual additions [51]	19
2.9	Key components of a floating photovoltaic system [54]	20
2.10	Efficiency comparison of PV technologies, at cell and module level [58]	21
2.11	Price Learning Curve by Technology [58]	22
2.12	Different types of floating structure [64] [51]	23
2.13	Forces acting on thin film PV system [66]	24
2.14	Battery comparison chart [71]	25
2.15	Stan Pontoon 9127, constructed by Damen Shipyards Group [78]	26
3.1	Ocean Sun's patented technology [64]	28
4.1	Overview of the system configuration without the use of battery system	34
4.2	Flow chart of the control logic for the configurations without batteries	35
4.3	Sizing methodology for the OFPV and electrolyzer capacities	36
4.4	Total system without batteries, modelled in Simulink	36
4.5	Overview of the system configuration using batteries	37
4.6	Electrolyzer load depending on the output of the FPV system, for the alkaline case.	38
4.7	Flow chart of the control logic of the battery	38
4.8	Battery control strategy model in Simulink	39

4.9	Total system with batteries model in Simulink	39
4.10	Overview of the floating PV model in Simulink	41
4.11	Overview of the DC-DC converter model in Simulink	42
4.12	Overview of the electrolyzer model in Simulink	42
4.13	Overview of the battery model in Simulink	43
4.14	Overview of the compressor subsystem in Simulink	44
4.15	Overview of the pipeline cost calculation in Simulink	45
4.16	Overview of the LCOH model in Simulink	46
5.1	Hydrogen Production in the alkaline system configuration with no battery addition	48
5.2	Total Subsystem Layout	50
5.3	Total System Layout	50
5.4	Contribution of system components to the LCOH	51
5.5	Sensitivity Analysis of the different values affecting the LCOH	54
5.6	Sensitivity Analysis of the FPV system Cost	54
7.1	Overview of the final system configuration	63
A.1	FPV Power Output depending on the different irradiance levels	76
A.2	Hydrogen Output for the configurations without batteries depending on the different irradiance levels.	77
B.1	FPV system power output in the alkaline system configuration with no battery addition	80
B.2	Electrolyzer load in the alkaline system configuration with no battery addition	80
B.3	Hydrogen Production in the alkaline system configuration with no battery addition	81
B.4	FPV System Power Output in the PEM system configuration with no battery addition	82
B.5	Electrolyzer load in the PEM system configuration with no battery addition	82
B.6	Hydrogen Production in the PEM system configuration with no battery addition	82
B.7	FPV System Power Output in the alkaline system configuration with batteries	83
B.8	Electrolyzer load in the alkaline system configuration with batteries	84
B.9	Battery state of charge (SoC) in the alkaline system configuration with batteries	84
B.10	Hydrogen Production in the alkaline system configuration with batteries	85
B.11	FPV System Power Output in the alkaline system configuration with batteries	86
B.12	Electrolyzer load in the PEM system configuration with batteries	86
B.13	Battery state of charge (SoC) in the alkaline system configuration with batteries	87
B.14	Hydrogen Production in the alkaline system configuration with batteries	87

LIST OF TABLES

1.1	Site information [16] [15] [14] [13]	6
2.1	Top green hydrogen projects announced [11]	10
2.2	Comparison between different technologies for water electrolysis [37] [25] [23] [38] [22] [6] [39]	15
2.3	Battery parameters [71] [75] [72] [76] [73] [74]	25
3.1	PV module parameters [61] [62] [59] [58] [60]	27
3.2	Costs for the OFPV system [61] [62] [59] [60] [84]	29
3.3	Electrolyzer parameters [42] [29] [42] [32]	31
3.4	Battery parameters [72] [76] [73] [74]	31
3.5	Compressor parameters [94] [42]	32
4.1	System Configurations	33
4.2	Energy produced from the FPV system	42
4.3	Battery Capacity for the different system configurations	43
4.4	Compressor Capacity for the different configurations	44
4.5	Pipeline properties for the different configurations	45
5.1	Results of the simulation for the four different configurations	47
5.2	Selected System Information	49
5.3	Subsystem Size	49
5.4	Sensitivity parameters for pessimistic and optimistic values	53
5.5	Scenario Data	55
7.1	LCOH of the four different configurations	62
A.1	Model Verification	76
A.2	Verification of the battery model	77
B.1	Results of the simulation for the configuration based on alkaline electrolysis without batteries	81
B.2	Results of the simulation for the configuration based on PEM electrolysis without batteries	83
B.3	Results of the simulation for the configuration based on alkaline electrolysis with batteries	85
B.4	Results of the simulation for the configuration based on PEM electrolysis with batteries	87

LIST OF ABBREVIATIONS

CAPEX	Capital Expenditure
CCS	Carbon Capture and Storage
DC	Direct Current
DoD	Depth of Discharge
FPV	Floating Photovoltaic
GHI	Global Horizontal Irradiance
HHV	High Heating Value
LCOE	Levelized Cost of Hydrogen
LCOH	Levelized Cost of Hydrogen
MEA	Membrane Electrode Assembly
MPPT	Maximum Power Point Tracker
OFPV	Offshore Floating Photovoltaic
OPEX	Operational Expenditure
PEM	Proton Exchange Membrane
PV	Photovoltaic
PV GIS	Photovoltaic Geographical Information System
STC	Standard Test Conditions
WACC	Weighted Average Cost of Capital

1

INTRODUCTION

1.1. MOTIVATION

Energy transition is one of the most important topics nowadays. Due to the Paris Agreement, which sets a general target of maintaining the average temperature of the world below 2 °C, several European countries have set goals to increase the renewable energy sources contribution in the energy mix [1]. However, renewable energy sources, cannot ensure a safe and reliable energy future, due to their variable power output caused by their dependency on the weather conditions. For example, sun is not shining during the night and winds are not strong all the time. Therefore, storage technologies are needed for clean and reliable energy systems to make optimal use of renewable energy sources.

Hydrogen has the potential to be a solution to this problem and become a fundamental part of future energy systems. Hydrogen is a simple and light chemical element and is capable of producing only water vapor from its combustion [2]. It provides the highest energy content per mass unit, with a higher heating value (HHV) of 39.42 kWh/kg [3]. Hydrogen cannot be found in its pure form in the nature and therefore a production procedure is required. Nowadays, hydrogen is mostly produced from fossil fuels representing the 95% of the hydrogen production worldwide. The rest 5% is produced from biomass-based procedures and water splitting [4]. The reason behind this extensive use of fossil fuels in hydrogen production is the relatively low levels of the fuel prices [5]. The production and consumption of hydrogen for 2019 is depicted in figure 1.1.

When hydrogen is produced from fossil fuels, named grey hydrogen, carbon dioxide is emitted to the atmosphere. In case carbon capture and storage (CCS) technology is used, the so-called blue hydrogen can be produced. Blue hydrogen can potentially be the bridging solution towards a clean and sustainable hydrogen production system. However, the cost of producing hydrogen with CCS technologies is high [7] and also, it does not represent a sustainable way of producing hydrogen. Therefore, other methods, based on renewable energy sources should lead the way in hydrogen production, such as water splitting or biomass-based technologies [5] [7]. In this case, it is called green hydrogen. The technology to produce green hydrogen from water splitting is called water electrolysis. In Water electrolysis, water is decomposed into oxygen and hydrogen

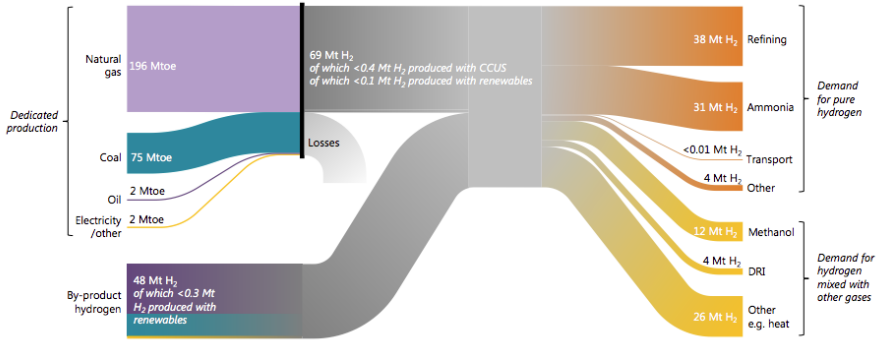


Figure 1.1: Hydrogen production and consumption in 2019 [6]

gases due to the application of electricity. This process takes place in a device named electrolyzer.

Coupling the electrolyzers with renewable energy sources is needed for clean and secure energy systems. Renewable energy sources' share in the energy mix is continuously increasing. Mostly wind and solar energy are used for the energy production, with other options to be hydropower, energy from biomass, geothermal energy, and wave and tidal energy [8]. However, hydrogen production from renewable energy sources is still negligible, mostly due to the high costs. The most cost-effective methods to produce hydrogen are based on fossil fuels (grey hydrogen), such as natural gas and coal. The cost of grey hydrogen production, especially when based on natural gas, are between 1-2 €/kg [6], but it can be higher depending on the region. Adding carbon capture storage technologies (CCS) makes hydrogen production more environmentally friendly, increasing however, the production costs to 1.5-2.5 €/kg [9]. Green hydrogen production based on renewable energy sources is currently higher, around 2-6 €/kg depending on the region. However, until 2030, the green hydrogen production costs are expected to drop to 1.5-3 €/kg [10] [9].

The global green hydrogen pipeline has already reached 207 GW, with projects being announced on a regular basis [11]. Most of the projects announced are intending for large scale, aiming to reduce the hydrogen production costs significantly. The leader of the announced projects is the HyDeal Ambition, which will be located in multiple sites in Western Europe and aims for 3.6 million tones per year of hydrogen production from 95 GW of solar energy which will be used to power 67 GW of water electrolysis. The plan is to deliver green hydrogen across Europe at a cost of 1.50 €/kg before 2030 [11]. In some countries, especially in Europe, it is extremely hard to find free land to harness renewable energy sources and therefore, attention is turned on offshore projects. A good example of such projects is the NorthH2, located in the northern part of the Netherlands, which will be based on energy produced from offshore wind with the target of one million tons of hydrogen production per year [11]. In general, the focus now is turn on large-scale hydrogen production, with most projects intend for more than one million tons of hydrogen production annually.

A significant portion of the announced projects are based on solar energy production. The sun is an unlimited energy source in the planet Earth and has the potential, theoretically at least, to cover the total global energy demand. However, in practice the presence of solar energy in the global energy supply mix is still small. The intensity of the solar irradiance differs between different locations and depends on various factors. The yearly average amount of solar energy that reaches the Earth's atmosphere is around 342 W/m^2 , of which 70% is available for use, since the rest 30% is scattered or reflected back to space [12]. As can be seen from figure 1.2, and focusing on Europe, the irradiance levels are higher in the southern part, with Spain, South Italy and Greece, being the optimal choice for a solar energy production.

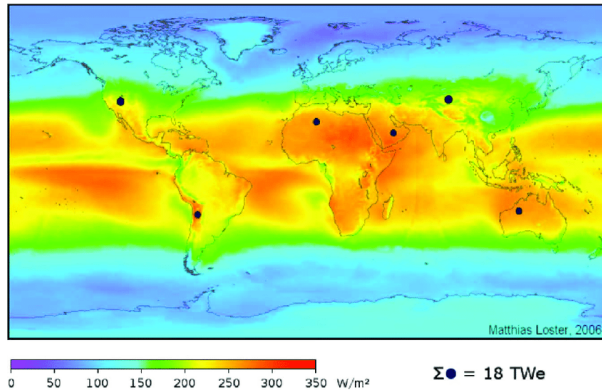


Figure 1.2: Global average solar irradiance [12]

1.2. AIM AND RESEARCH QUESTIONS

Overall, hydrogen production from large scale solar farms, along with large scale hydrogen transport through pipelines can lead to low hydrogen production costs and ensure a reliable and clean energy future. Considering European countries, free areas are difficult to find for large-scale installations, and therefore, offshore projects have the potential to become a great option. The most optimal locations for solar energy, as already indicated, are in the South part of Europe. Therefore, this research, aims to evaluate the technical and financial feasibility of a large-scale offshore power to hydrogen plant by 2030, based on offshore floating solar energy, located northern to Crete, in the Aegean Sea, in Greece. The hydrogen produced will be injected into the main hydrogen network and distributed across Europe. Therefore, the main research question is:

What is the cost of producing 1 million tons of hydrogen per year from floating solar energy, in an area north of Crete?

1.2.1. SUB-QUESTIONS

The following sub-questions will be elaborated, in order to assist in reaching a conclusive answer to the main research question:

1. What are the main system components of an offshore solar to hydrogen system?



Figure 1.4: Depth variation along with the distance from shore for the selected location [13]

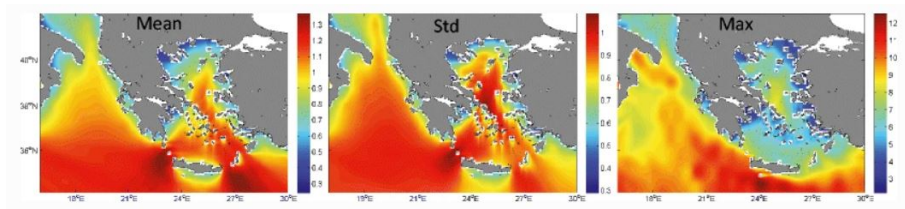


Figure 1.5: Mean Significant Wave Height (SWH), standard deviation of SWH, maximum SWH in meters, respectively [15]

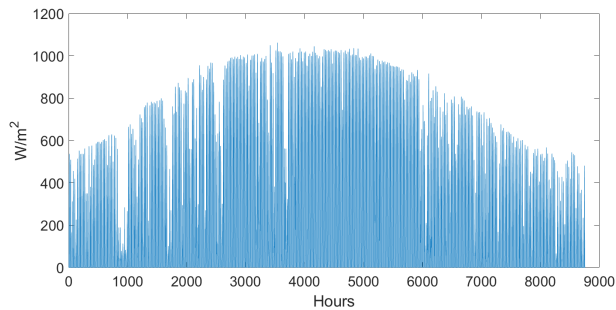


Figure 1.6: Irradiance data for a typical meteorological year [16]

It should be highlighted, that data for sea water areas were not available and therefore, the data used refer to the closest shore area, assuming that the difference is not significantly affecting the results. By noticing the figure, it can be understood, that the irradiance depends highly on the season of the year. During the winter hours, the irradiance levels are lower, while during the summer hours they are higher. The spikes in the graph represent high irradiance levels, while the dips represent the low irradiance periods, including the night hours. Overall, the location details are presented in table 1.1:

Table 1.1: Site information [16] [15] [14] [13]

Coordinates	35.47° N, 24.78° E	
Distance from shore	15	km
Water Depth	1000	m
Average Global Horizontal Irradiation	1810	kWh/ m^2
Specific photovoltaic power output	1610	kWh/ KW_p
Average Temperature	19.5	$^{\circ}$
Mean Significant Wave Height	1.5	m
Max Significant Wave Height	7	m

1.3.2. SYSTEM LAYOUT

After addressing the main location characteristics, the system components of the off-shore solar to hydrogen system need to be identified. The hydrogen production is based on electricity produced from an offshore floating photovoltaic system. Like all renewable energy sources, PV systems are characterized by a fluctuated energy production, as can be seen from figure 1.6. This becomes even clearer by focusing on a single week of the year, as presented in figure 1.7. More specifically, the irradiance levels deviate significantly, not only during the whole week, but even during the same day.

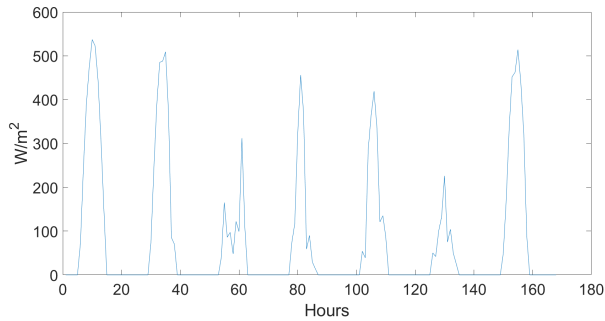


Figure 1.7: Irradiance data for a single week of the year [16]

Direct coupling of electrolyzers with renewable energy sources is questioned through the literature. The coupling of electrolysis systems to renewable energy sources is feasible in technical terms [18]. In practice, large-scale electrolysis systems include several individual stacks in parallel. Therefore, the power consumption of the electrolyzers can be controlled by switching off individual electrolyzer stacks [19]. Power electronics, are needed to adjust the current and voltages to the operating level of the electrolyzer. However, dynamic operation of the electrolyzers, if not controlled properly, can hide dangers regarding the efficiency of the system and hydrogen quality [20]. To prevent such issues, a battery could buffer the PV power output making the electrolyzer operation more stable. Batteries can also achieve higher energy usage, by using the extra energy during the

day and provide it to the electrolyzer to operate during the night. Therefore, the battery addition to the system should be examined.

The electrolyzer unit requires pure water to operate. Therefore, a water treatment unit based on reverse osmosis is needed. The produced hydrogen will be injected into the hydrogen network. To do so, the hydrogen should be pressurized to 100 bar. Therefore, a compressor facility to increase the pressure from the electrolyzer output to 100 bars is needed. The system is autonomous, which means that there is no connection to the electricity grid, and all the energy used, is generated by the OFPV system. Therefore, the electricity for all other services must be sourced either from the FPV system or from a temporary storage system, such as a battery. The reverse osmosis facility and the hydrogen compressors, need to operate only when the electrolyzer operates. So, their electricity needs will be covered from the OFPV system and if needed, from a temporary storage method. On the other hand, there are facilities such as the computer and control systems for the electrolyzers, that should operate during the night hours. Therefore, a small number of batteries will be used for this purpose also. An overview of the system can be seen in figure 1.8.

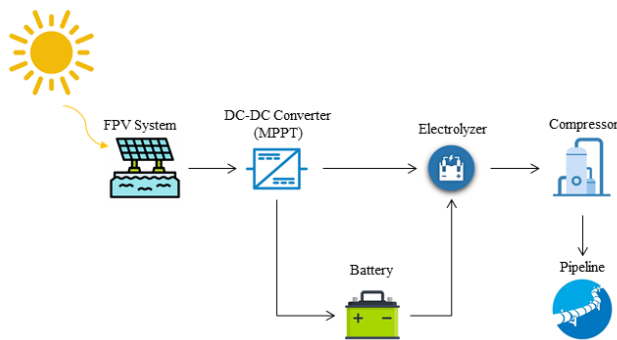


Figure 1.8: Overview of the system configuration

After addressing the main system components, a literature review needs to be performed, in order to identify the main challenges behind offshore hydrogen and offshore floating solar systems. In addition, information about the costs and the sizing of the different components are needed. At this point, after knowledge is already built, the model will be designed on Matlab and Simulink software. The output of this model, is the levelized cost of hydrogen (LCOH), which will show what is the economic feasibility of the project.

1.4. REPORT STRUCTURE

In Chapter 2, background information on green hydrogen projects, hydrogen production systems, electrolyzers and the floating PV technologies will be presented. In Chapter 3, the basics of the system design will be analyzed, including information about the loca-

tion and the sizing of the different components. Chapter 4, presents the models created for the system in Matlab and Simulink software. In Chapter 5, the final results will be addressed and the final system configuration will be decided. Discussion will take place in Chapter 6, along with sensitivity analysis results. In the last chapter, chapter 7, the conclusions of this research are addressed and recommendations for future research are given.

2

LITERATURE REVIEW

In this chapter, literature material relevant to the proposed offshore hydrogen production system based on floating solar energy will be presented. At first, the overview of the hydrogen projects will be illustrated. Then all relevant literature information for the components of the proposed hydrogen system will be addressed.

2.1. HYDROGEN

2.1.1. HYDROGEN PROJECT PIPELINE

Currently, there are 228 hydrogen projects worldwide across the value chain, as can be seen in figure 2.1 [21]. 17 out of this, are already-announced GW-scale production projects, with the biggest in Europe, Australia, the Middle East and Chile.

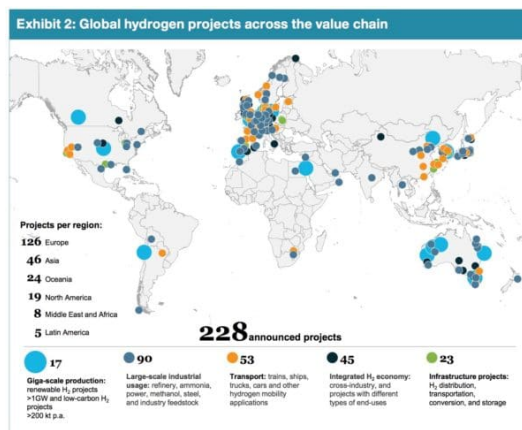


Figure 2.1: Hydrogen projects worldwide [21]

The global green hydrogen pipeline has already reached 207 GW, with projects be-

ing announced on a regular basis [11]. Currently, the electrolyzer market is still at an early stage. Most projects are in MW scale, with projects up to 20 MW, being the norm, while projects up to 250 MW are already announced. Most of the projects announced are intending for large scale, aiming to reduce the hydrogen production costs significantly. The key projects for green hydrogen production worldwide are summarized in the following table:

Table 2.1: Top green hydrogen projects announced [11]

Name	Location	Power Source	Electrolyzer Capacity [GW]	Hydrogen Output [m tones/year]
HyDeal Ambition	Western Europe	Solar (95 GW)	67	3.6
Unnamed	Kazakhstan	Wind & Solar (45 GW)	30	3
Unnamed	Aman	Wind & Solar (30 GW)	16-20	Not stated
Unnamed	Oman	Wind & Solar (25 GW)	14	Not stated
Asian Renewable Energy Hub	Western Australia	Wind (16 GW) & Solar (10 GW)	14	1.75
NorthH2	northern Netherlands	Offshore wind	10	1

2.1.2. WATER ELECTROLYSIS

Most of the green hydrogen projects are based on water electrolysis. Water electrolysis is a hydrogen production method, which when based on renewable energy sources, has the potential to produce green hydrogen without harmful emissions. Water electrolysis is used for more than 100 years, but recently, it has gained increased interest. The basic principle of water electrolysis is the separation of water into oxygen and hydrogen gases due to the application of a direct current. The system in which this procedure takes place is called an electrolyzer and consists of multiple electrolysis cells, each one of which consists of two electrodes (anode, cathode), an electrolyte and a membrane or diaphragm, which prevents the recombination of hydrogen and oxygen molecules. The two electrodes are connected to an external power supply and must be resilient to corrosion and have great electric conductivity [22] [23].

The chemical reaction of water electrolysis is [22]:



In the electrolysis process, the electrons leave the anode, polarizing positively this electrode, and the oxidation half-reaction takes place. Then, the electrons flow to the

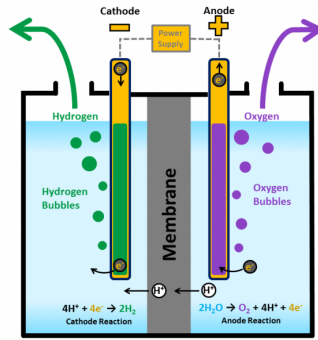


Figure 2.2: Basic electrolytic cell for water electrolysis [24]

cathode, polarizing this electrode negatively, and the reduction half-reaction takes place. Therefore, the oxygen is generated at the anode and the hydrogen at the cathode [22] [25].

The energy of the water electrolysis procedure is given by the enthalpy of the process, with constant pressure and temperature. Therefore, the theoretical energy need for the previous reaction to take place, is the difference in the enthalpy, ΔH . According to the thermodynamic laws, this difference is [22]:

$$\Delta H = \Delta G + T \Delta S \quad (2.2)$$

In the previous equation, ΔG (reversible part) corresponds to Gibbs free energy, ΔS is the entropy and T the absolute temperature (reversible part). ΔG is provided as electrical energy while $T \Delta S$ is supplied as thermal energy. In the process of Water electrolysis, a theoretical minimum of 237 kJ of electrical energy is needed in order to split each mole of water and energy to overpass the difference in entropy. Thus, the minimum theoretical value of the reaction is 285.8 kJ per mol with no external energy input [26]. However, the actual energy needed for water electrolysis is bigger because of current and overvoltage losses [4].

Although there are several water electrolysis technologies available, such as alkaline water electrolysis (AWE), proton exchange membranes (PEM), solid oxide water electrolysis (SOCE) and anion exchange membrane electrolysis (AEM), the only ones available commercially at a large scale are alkaline and PEM, and they will both be examined. The performance of electrolyzers depends on many factors, such as voltage, current, pressure, temperature, electrode spacing, and electrolyte concentration. However, these factors will not be examined in this report, as the target is to examine the electrolyzer as a part of a hydrogen production system and not to investigate the fundamentals of water electrolysis technologies.

ALKALINE WATER ELECTROLYSIS

Alkaline water electrolysis is the most common method of water electrolysis, as it is mature in the market and relatively cheap, compared to the other methods. In this technology, the electrolyzer cell consists of two electrodes separated by a diaphragm, made

from asbestos [23], in order to keep separated the produced hydrogen at the cathode from the produced oxygen at the anode. The electrolyte in this case, is a highly concentrated aqueous solution of potassium hydroxide (KOH), with concentration around 25–30 wt.%. However, there are also other possible electrolytes such as sodium hydroxide (NaOH) or Sodium Chloride (NaCl) used. Water is introduced at the cathode, where it is split into hydrogen and hydroxide ions [22]. The operating principle of alkaline water electrolysis is depicted in figure 2.3.

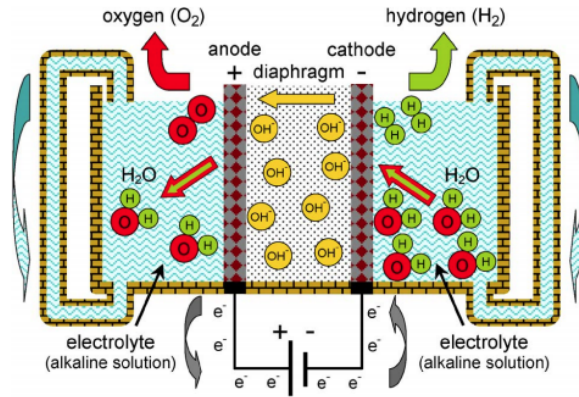
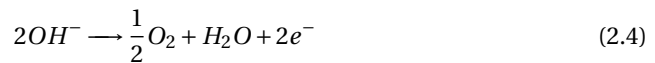


Figure 2.3: Operating principle of alkaline water electrolysis [22]

The half reaction of the cathode in alkaline electrolysis is [22]:



The half reaction of the anode is:



The current density of alkaline electrolyzers ranges between 0.2 and 0.4 A/cm^2 , while the output pressure can be up to 30 bars. The purity levels of the produced hydrogen reach 99%. Water with low purity levels is needed for both types of electrolyzers, and therefore, water treatment facilities are needed. For alkaline electrolyzers the water electrical conductivity should be 5 S/cm . The efficiency of electrolyzers is not constant, taking values depending on the input load. The efficiency of alkaline electrolyzers can taking values from 64 to 84 % according to different literature sources [7] [27] [5]. The footprint of the electrolyzer is a very important parameter, especially for offshore systems. However, for large scale projects, it is not clearly declared in the literature. Given the fact that, only MW scale projects are active, only estimates can be given about this value. An electrolyzer facility, apart from the electrolyzer units, includes the water treatment facility, the electrical equipment, such as converters from AC to DC, the compression units and the control rooms and offices [28]. According to IEA, the footprint of an

alkaline electrolyzer plant is $0.095 \text{ m}^2/\text{kW}$ [29]. Hydrogen Europe indicates that the footprint of alkaline electrolyzers will be reduced from 0.08 currently to $0.04 \text{ m}^2/\text{kW}$ by 2030 [30]. Institute for Sustainable Process Technology (ISPT) presented a study which aims to present blueprints for future GW water electrolysis facilities. In this report, it is stated that a GW alkaline electrolyzer facility has a footprint of $170,000 \text{ m}^2$ ($0.17 \text{ m}^2/\text{kW}$) with the possibility to be reduced to $100,000$ [28]. Weight is an equally important parameter. However, also in this case, there is not a standard weight for electrolyzer facilities and estimations will be used. From comparing available technical specifications of different commercial models, the specific weight of alkaline electrolyzers is $0.02\text{-}0.03 \text{ kg/W}$ [31].

The minimum part load operation value is 10% of the rated capacity for alkaline electrolyzers, meaning that below this level the electrolyzer is shut down, for safety reasons [32]. The cold start-up time, is reported to be 20 minutes [33] and warm start-up time less than 5 minutes [19] for alkaline electrolyzers. Alkaline electrolyzers are reported to have a ramping level of 20% (full load)/second by 2030 [33], meaning that they are able to adjust the power demand in seconds. In some cases, alkaline electrolyzers are not preferred for coupling with renewable energy sources, therefore, their use is more optimal with constant power supply. However, for cases like Greece, where the fluctuation of solar energy is not so intense compared to northern European countries, alkaline electrolyzers can be used effectively.

In terms of cost, alkaline water electrolyzers are cheaper than the other technologies, since expensive metals are not required, and non-platinum group metal (non-PGM) catalysts are used. Currently, the alkaline electrolyzer costs are high ($>500 \text{ €/kW}$), but there are projections that massive electrolyzer production will reduce the costs further.

PROTON EXCHANGE MEMBRANE (PEM) WATER ELECTROLYSIS

Proton exchange membrane (PEM) electrolyzers use a membrane instead of a diaphragm that alkaline use. The water is imported at the anode where it is separated into protons which penetrate through the membrane to the cathode to produce hydrogen, while oxygen remains back with water. At the anode, water is oxidized to create oxygen, electrons, and protons. The anode, cathode, and membrane set constitute the membrane electrode assembly (MEA) [22].

The half reaction of the cathode in alkaline electrolysis is [22]:



The half reaction of the anode is:



PEM electrolyzers are also a mature technology, with extended use in the market. The current density of PEM electrolyzers is $0.6\text{-}2.0 \text{ A/cm}^2$, much higher than the one of alkaline electrolyzers, meaning that less space is needed for hydrogen production. PEM hydrogen output is better in terms of purity compared to alkaline, reaching 99.9%. For alkaline electrolyzers the water electrical conductivity should be 1 S/cm . The efficiency of PEM electrolyzers can taking values from 65 to 80% according to different literature

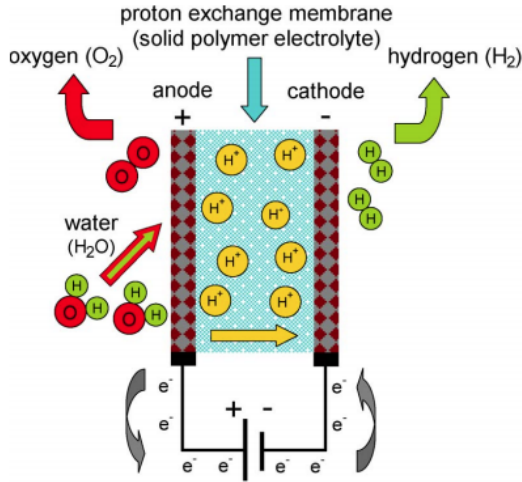


Figure 2.4: Operating principle of PEM water electrolysis [22]

sources [7] [27] [5]. Like in the alkaline case, PEM electrolyzer footprint is not specified in the literature for large scale projects. It is reported to be half ($0.048 \text{ m}^2/\text{kW}$) comparing it to alkaline [29]. Hydrogen Europe projects that footprint of PEM electrolyzers will be reduced from 0.05 to $0.025 \text{ m}^2/\text{kW}$ [30]. ISPT states that PEM electrolyzer footprint for a GW facility is $130,000 \text{ m}^2$ and can be further reduced to $80,000 \text{ m}^2$ [28]. The specific weight of PEM electrolyzers is reported to be approximately 0.01 - 0.02 kg/W , almost three times lower than the one of alkaline [34] [35].

The minimum part load operation value for PEM electrolyzers can be between 0 and 5% [32]. The cold start-up time, is reported to be up to 5 minutes and warm start-up time a few seconds for PEM electrolyzers [33] [30]. PEM electrolyzers are reported to have a ramping level of 40% (full load)/second by 2030 [33]. PEM respond quickly to varying power supply, and therefore, they can be used on a wide range of applications, including direct coupling with renewable energy sources. The cost of PEM electrolyzers is almost double than the one of alkaline at the moment. However massive production and larger scale use in projects could possibly reduce the costs by more than half [36].

An overview of the key characteristics of both alkaline and PEM electrolyzers are presented in table 2.2:

Table 2.2: Comparison between different technologies for water electrolysis [37] [25] [23] [38] [22] [6] [39]

	Alkaline	PEM
Electrolyte	Aq. potassium hydroxide (20–30 wt% KOH)	Polymer membrane (Nafion)
Current density [A/cm ²]	0.2-0.4	0.6-2.0
Gas Purity [%]	99	99.99
T _{operating} [°C]	60-80	50-80
Operating Pressure [bar]	1-30	30-80
Stack Lifetime [1,000 h]	60-90	30-90
Efficiency [%]	65-84	65-80
Maturity	Mature	Mature
Water Electrical Conductivity [S/cm]	5	1
Cold Start-Up Time [Minutes]	20	5
Warm Start-Up Time [Minutes]	5	Few Seconds
Min Part Load Operation [%]	10	0-5
Footprint [m ² /kW]	0.04-0.17	0.025-0.13
Weight [kg/W]	0.02-0.03	0.01-0.02
Capital Cost [€/kW _{el}]	500-1,400	1,100-1,800
Advantages	Low cost, long lifetime, mature technology, high efficiency	High current densities, fast system response, no corrosive substances, high-purity H ₂
Disadvantages	Low efficiency, low current densities, corrosive character, slow response	High cost, shorter lifetime

2.1.3. REVERSE OSMOSIS

Most electrolyzer technologies cannot operate on sea water. Therefore, clean water with low conductivity is required for the electrolysis process. To reach the desirable level of conductivity, specific treatment is needed, such as desalination and purification pro-

cesses. Reverse osmosis is the most commonly used technology for water purification. It is based on the application of high pressure in order to ensure separation of water and dissolved substances [40] [41]. The reverse osmosis plant needs 9 litres of water to produce 1 kg of hydrogen [42]. The power consumption of a reverse osmosis facility is 3 kWh/m^3 [43]. The capital cost of a reverse osmosis unit is expected to fall to around 1,100 $\text{€}/(m^3/d)$ by 2030 [44].

2.1.4. HYDROGEN STORAGE & TRANSPORT

Hydrogen storage, transmission and distribution are key elements in the hydrogen value chain. Hydrogen has a very low energy density, thus, storing it requires compression or binding it to specific materials [3] [39]. The most common methods for hydrogen storage are compressed gas storage, liquid storage and solid storage in metal hydrides.

Apart from hydrogen storage, transmission and distribution is a crucial issue to the extended hydrogen use in energy systems. The main methods for delivering hydrogen are in liquid form in cryogenic tanks or in gaseous form by either compressed pressure vessels contained in tube trailers or through gas pipelines. In case hydrogen is used in large scale, the pipeline network can be an option with great potential, since the costs are significantly lower than the other types of transport. A huge amount of dedicated hydrogen pipeline is then needed, which requires high level of investment [5] [45]. Their size varies from 6-48 inches in diameter, depending on their use [46]. The global hydrogen pipeline network exceeds 4,500 km (2016 data), as presented in [39]. A hydrogen pipeline network can potentially offer the most cost-beneficial way of energy transport. More specifically, and comparing to electricity, pipelines can distribute ten times the energy at eight times lower costs than the cables [39]. Furthermore, hydrogen pipelines' lifetime is higher than the one of electricity cables. For these reasons, hydrogen transport through pipelines is selected as the distribution method in the proposed system.

2.2. SOLAR ENERGY

Hydrogen production from renewable energy sources is getting increased attention lately for several reasons. One of them is that, over the last years, the levelized cost of energy (LCOE) has dropped sharply, as can be seen in figure 2.5. From this figure, one can notice that the LCOE of solar energy has dropped to less than 0.1 \$/kWh in the latest auctions.

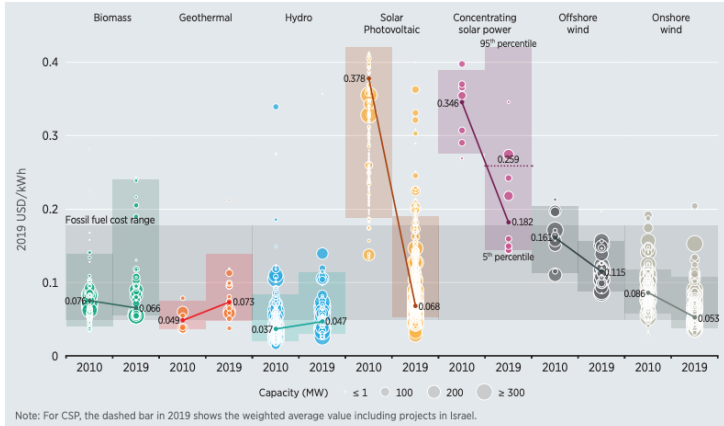


Figure 2.5: LCOE for different renewable energy sources (2019 data) [47]

Solar energy is one of the main power sources in green hydrogen projects. In this section, the main background information on PV technologies and systems will be presented, along with relevant to this research information about floating technologies and structures.

2.2.1. PHOTOVOLTAIC BASICS

Solar cells, made of semiconductor materials, such as silicon (Si) or germanium (Ge), make use of the photovoltaic effect, releasing electrons when exposed to sunlight to produce direct current (DC) electricity. The photovoltaic (PV) effect is voltage generation at the junction of two different materials due to exposure to sunlight [48].

Several series of solar cells interconnected form a PV module. There are several technologies available in the market, such as poly- and mono-crystalline silicon, amorphous silicon, thin film and others. The most used type of modules are the crystalline silicon, which usually consist of 60 to 72 solar cells. Apart from the modules, a PV system includes also other equipment, such as cables, wires, switches, automatic protection equipment, fuses, racking, mounting structure and others [48].

The parameters that characterize PV modules are measured under standard test conditions (STC). In other words, the total irradiance on the solar cell is 1000 W/m^2 , the spectrum should be as the Air Mass 1.5 spectrum and the temperature of the solar cell should be equal to 25°C [48]. The behavior of an illuminated solar cell can be elaborated by an I-V curve, which is depicted in figure 2.6. The I-V curve represents all the possible combinations of current and voltage output of a solar cell. The main parameters that are used to describe the performance of solar cells are the peak power P_{MP} , which is

the rated capacity of the module, the short circuit current I_{SC} , which reflects the current when terminals of the PV module directly connected to each other such that the voltage breaks down, the open circuit voltage V_{OC} , which is the voltage when no current exists and the fill factor FF which is the maximum power produced by a solar cell divided by the product of V_{OC} with I_{SC} .

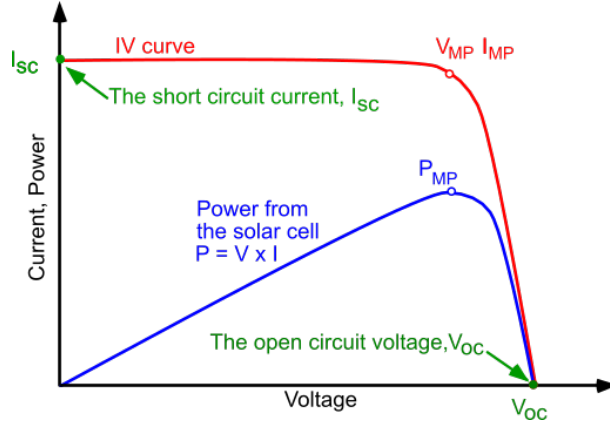


Figure 2.6: Characteristic I-V curve of a PV module [49]

The I-V curve depends on the module temperature and on the irradiance, which means that the PV module will have a unique I-V curve and a new maximum power point (P_{MP}). In order to make optimal use of the PV module, this point needs to be identified. For this reason, maximum power point trackers (MPPT) are used, which is nothing more than an algorithm usually embedded in the inverter [48].

2.2.2. FLOATING PHOTOVOLTAIC SYSTEMS

Photovoltaic (PV) modules can be installed in various layouts, both onshore and offshore. Onshore solar PV can be installed either on the ground, as large, utility-scale power plants, or on roofs of residential or commercial buildings. Both installations, require space, which is not always free and available, therefore, other solutions are considered, such as setting PV modules on the top of the canal [50].

All the layouts presented above, are installations that require the use of land, which is hard to find in many countries and there is usually a conflict for other possible uses such as agricultural activities. To overcome this obstacle, floating solar systems can offer great potential. Floating photovoltaic (FPV) technologies (figure 2.7) have gained increased interest in the market lately and they seem to provide an appealing solution. This technology is very important for countries with land availability issues such as Japan, Singapore, Korea, Philippines, and many others. FPV systems can be installed in several water areas, such as oceans, lakes, reservoirs, wastewater treatment facilities, canals and others [51].

Currently, most of FPV applications take place on inland water bodies, although oceans cover about 70% of the Earth's surface. The reason behind this, is that there are several important challenges in offshore FPV installations, such as extreme water sur-



(a) Floating PV system installed by Akuo Energy in France [52]



(b) Offshore floating PV system installed by Oceans of Energy in the North Sea [53]

Figure 2.7: Floating PV plants

face conditions, stronger winds, and larger waves. The first FPV system was built in 2007 in Aichi, Japan. The first commercial application of FPV is a 175 kWp system set up at the Far Niente Winery, California, United States, in 2008. According to the World Bank, and as can be noticed in figure 2.8, there was a significant increase in the last years in cumulative installed capacity of FPV projects worldwide, from 169 MWp in 2016 to 1314 MWp in 2018 [51]. The majority of FPV installations take place on inland waters.

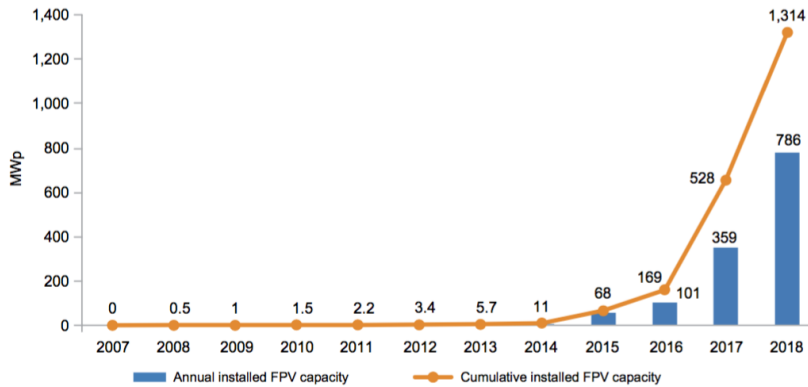


Figure 2.8: Global installed FPV capacity and annual additions [51]

FPV systems offer important benefits in comparison to land-based PV systems. Firstly, they take advantage of unusable space, which is very important for several countries. In addition, in some cases, FPV systems offer higher efficiency than ground-based PV systems due to the lower temperature levels of the water environment. Finally, other advantages of FPV systems include reduced algae growth and reduced water evaporation [50] [51]. However, there are important challenges that need to be considered. The moisture environment of the installation can affect the performance of the modules as well as the floating structure. In addition, offshore FPV systems should be able to withstand rougher environmental conditions such as floods, cyclones, waves, and heavy winds, something

that increases the cost and the uncertainty of the structure.

The parts that a PV system consist of are presented in figure 2.9. More specifically, the main part is the PV modules, which are mounted on a floating platform. The anchoring and mooring system is responsible for keeping the plant in the desired position. Inverters are also used, which can be placed on shore in some cases, and finally, there are cables in order to transfer the produced energy to the shore [54].

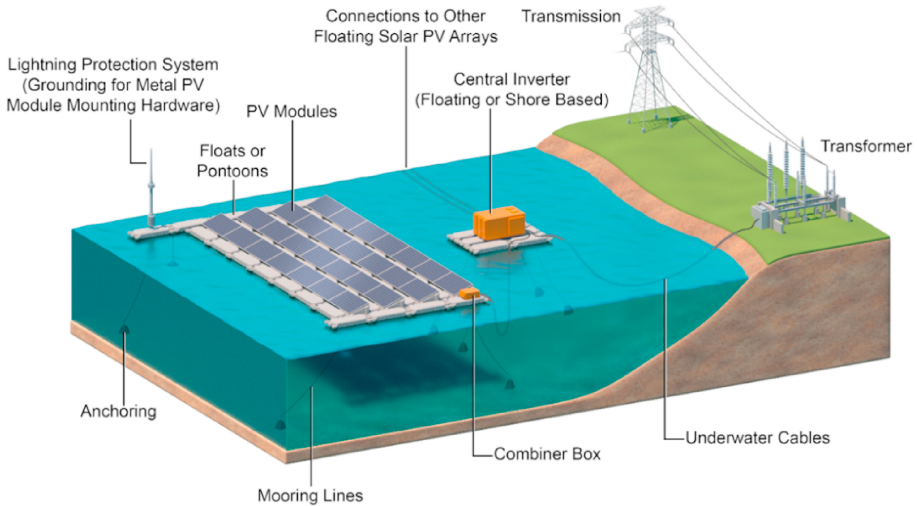


Figure 2.9: Key components of a floating photovoltaic system [54]

The system proposed in this research is an offshore floating PV system. Offshore environments represent a great option for renewable energy and therefore, it is important to investigate the challenges related to designing and installing FPV systems in marine environments [55]. The main advantages of offshore FPV are mostly the same with the inland FPV systems, offering the use of unexploited area and potentially higher efficiencies, due to the lower temperatures further offshore. However, further offshore, the environment is highly demanding and therefore it should be ensured, that the system will survive in harsh conditions, such as strong waves, wind and current loads. Degradation due to saltwater corrosion and soiling losses from bird droppings are also an important factor that should be considered in offshore FPV.

Furthermore, the project designed in this research, configuration differs from a typical FPV system illustrated in figure 2.9 also in other details. More specifically, there is no need for alternate current (AC), therefore, inverters are not included. Instead, since electrolyzers require a different specific voltage to operate, which usually differs from the output voltage of the FPV system, DC-DC converters are needed in order to regulate the voltage and current. A DC-DC converter is a device used to regulate the input voltage and current [56].

2.2.3. FPV SYSTEM COMPONENTS

In this section, background information on the different components of a floating PV system will be presented.

SOLAR PV MODULES

In general, there are two main types of PV panels, rigid and flexible. The selection of the type of solar modules depends on several factors such as space, cost, relative humidity, and type of water bodies. The type of panels selected significantly affects the rest of the system components. For instance, flexible panels may not require a floating structure to buoy in the water. The main PV technologies on the market are silicon based and thin film technologies [57].

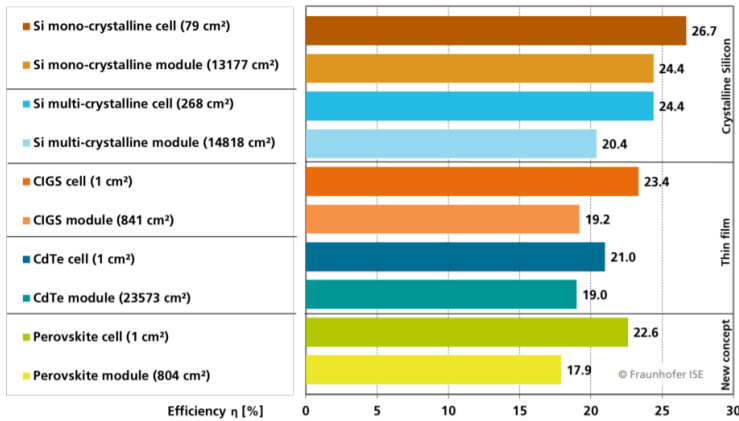


Figure 2.10: Efficiency comparison of PV technologies, at cell and module level [58]

Among the different technologies in the market, mono-crystalline silicon PV modules perform the highest efficiency values. The efficiency of the PV cells and modules in the lab is depicted in figure 2.10. In the laboratory, the modules with the higher efficiency are based on mono-crystalline silicon with 24.4%. The highest lab efficiency for thin film technology modules is 19.2% for CIGS and 19% for CdTe. Finally, record lab module efficiency for Perovskite is 17.9% [58]. According to Fraunhofer ISE [59], the average crystalline silicon PV module efficiency in the past ten years raised approximately by 0.4% per year. Assuming that this development will be continued [60], the average module efficiency by 2030 is assumed to be increased from 17.2 % (2018) to 22%. Glass-glass modules are usually selected for floating applications due to their higher resistance to internal corrosion [55].

In terms of costs, according to Fraunhofer ISE, the price of crystalline silicon PV modules is approximately 0.2 €/Wp and for thin film slightly higher for 2020, as can be noticed in figure 2.11 [58]. The average spot price of mono-crystalline and thin film PV modules is approximately 0.19 €/Wp [61]. However, following the learning rates, the price of PV modules is projected to drop even more. The projections for 2030 estimate that the price of the c-Si modules will be in the range between 0.11-0.19 €/Wp [62].

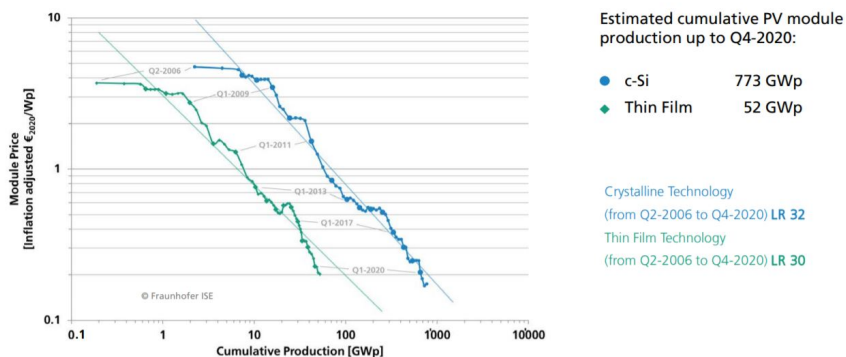


Figure 2.11: Price Learning Curve by Technology [58]

FLOATING STRUCTURES

Floating photovoltaic systems is a relatively new technology, and therefore, the area lacks technology convergence on the floating structure types. Some of the most used structures are separate floats, galvanized steel frames and membranes, which are used to provide buoyancy to rigid PV panels.

The main type of structures used in FPV systems is separate floats, made of high-density polyethylene (HDPE), which support the modules. Secondary floats are also added between the modules, for maintenance purposes and to prevent mutual shading. The main advantage of this technology is the easy installation process. In addition, since the floaters are connected between each other through bolts or pins, makes scaling up the structure a simple procedure. On the other hand, such structures cannot withstand strong waves and therefore, are not appropriate for offshore projects [51] [63].

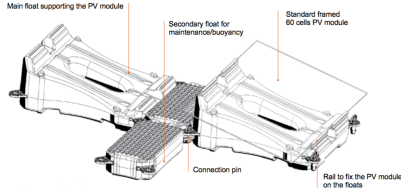
A different option is to use metal pipes to support PV panels and connect the structures to pontoons, to provide buoyancy. This design is a simpler concept than the pure floats, since pipes are more easily available in the market. However, such structures, have several metal parts and mechanical connections, and therefore are more vulnerable to wave forces. This structure, is also proffered for inland waters, with less powerful waves active [63] [51].

Another type of platform is floating membranes, which provide the base for the PV panel installation. Ocean Sun, a Norwegian company, offers a solution of such structures, where a membrane is fixed to a buoyant ring. This system has been used for fish farm applications in Norway and it can also be used for offshore applications as well. According to Ocean Sun, this structure has the ability to increase the energy yield due to the direct contact of the membrane with water [51] [64].

Finally, another type of structure suitable for offshore projects was proposed in 2019 by Oceans of Energy. More specifically, they installed multiple interconnected pontoons with solar modules mounted on top of it. This was the first offshore PV project in the world. The installed capacity started at 8.5 kW and now it is expanded to 18 kWp, with plans to be further expanded to 50 kWp. The platform is a big pontoon, with solar mod-

ules installed horizontally on it. Until now, the platform managed to survive rough sea conditions, withstanding wind speeds up to 120 km/h and waves with height up to 5 meters. The system proposed by Oceans of Energy is designed to withstand waves of up to 13 meters and it is planned to reach 1 MWp of installed capacity through 2021.

All the different types of structures can be seen in figure 2.12:



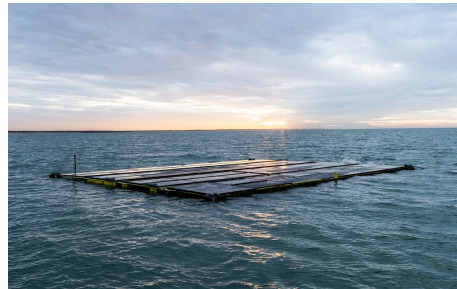
(a) Floats from Ciel & Terre International



(b) Floats and Metal frames from Scotra



(c) Membrane by Ocean Sun - Kyrholmen Project



(d) Offshore FPV system designed and installed by Oceans of Energy [53]

Figure 2.12: Different types of floating structure [64] [51]

FLEXIBLE SYSTEMS

In flexible systems, thin film PV technology is used and usually no support structure is needed. This technology can easily adapt and reform with the wave motion due to the light weight, as depicted in in figure 2.13. Thin film FPV systems are cheaper than the ones based on rigid panels due to the fact that a pontoon or floating structure is not always required. In addition, the direct contact with the water provides self-cooling and self-cleaning from dust and bird droppings [65]. However, thin film PV modules have lower efficiency than most of the rigid panels.

Thin film technology is a good option for offshore plants for several reasons. Firstly, less maintenance is needed due to the fact that this type of system requires less components. In addition, in offshore projects, there are important environmental forces that should be considered as presented in figure 2.13. In case pontoons or metal structures are used in offshore systems, they would be highly affected from these forces. However, thin film technology based FPV systems have less wave energy interaction, reducing the force on the mooring system, making them more appropriate for offshore installations. However, there are some important issues regarding this type of FPV systems, such as the electrical safety. Since electrical equipment is usually in direct contact with water,

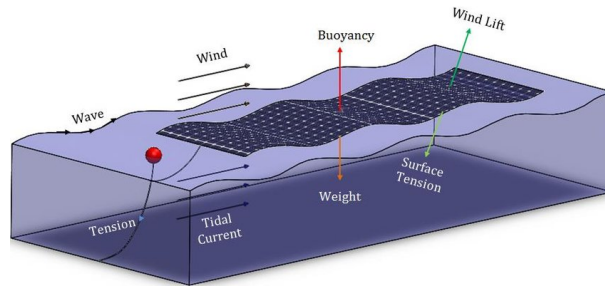


Figure 2.13: Forces acting on thin film PV system [66]

it should be resistant to moisture and corrosion. In addition, another very significant challenge for such systems, is bio-fouling [51] [67].

MOORING & ANCHORING

The mooring and anchoring systems are responsible to prevent free movement of the floating PV and to fix it in a specific position, withstanding waves and wind loads. For inland waters, bottom anchoring, bank anchoring and anchoring with piles are the main techniques selected. In the offshore industry, the selection of anchors follows the proven practices used extensively in the oil and gas industry. There are several types of anchors in the offshore industry, the most common of which are dead-weight anchors, drag-embedded anchors and anchoring with piles [68]. The selection of the proper type depends on the location and the relevant situation, such as water depth, soil conditions, and variation on the level of the water [51].

Mooring lines are also an essential part of the anchoring system. The primary types of mooring lines used for offshore structures, are chains, ropes and synthetic fiber ropes. Mooring lines should be loose enough to handle stress levels and changes in water level, but not in a level that allows extensive movement of the system [51]. The main types of mooring systems used for offshore projects are catenary, taut and compliant mooring systems. Taut and compliant/hybrid systems are more appropriate for offshore installations that catenary systems, since they have shorter mooring lines and require less seafloor[69].

2.3. BATTERIES

Due to the large fluctuations of solar power, a battery can serve as an instantaneous and daily energy buffer for storing the excess energy of the PV system. The battery bank makes the electrolyzer input smoother and can keep the electrolyzer operating during the night. Lead acid and lithium ion are the main types of batteries used in energy projects. Lead acid batteries are relatively cheap compared to the other types; however, they require regular maintenance and they also have a low depth of discharge, meaning that they need to be charged more often [70]. Lithium-ion batteries are used in electric vehicles (EV), something that made them quickly one of the most widely used types. They offer great advantages in comparison to lead acid, such as the lack of maintenance needed, higher energy density (figure 2.14) and longer life cycle. The main problem of

lithium-ion batteries is related to their cost, as they are very expensive at the moment. However, their costs are projected to decline in the future.

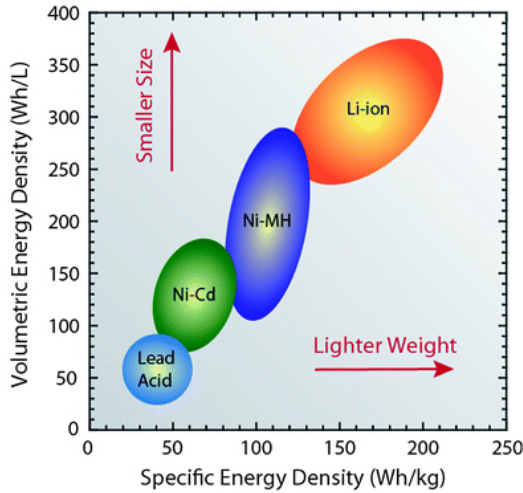


Figure 2.14: Battery comparison chart [71]

One of the most important parameters is the depth of discharge (DoD), which shows the level of charging/ discharging for a battery. If the battery is discharged beyond its DoD, this may result to degradation and reduced cycle life. The DoD for lithium-ion batteries is reported to be higher than 90%, while for lead-acid batteries is between 50 and 75 %. The round-trip efficiency of lithium-ion batteries is 90-95 % and for lead-acid 85-90%. Finally, in terms of costs, lead-acid batteries is the clear winner, as can be seen in table 3.4 [72] [73] [74].

Table 2.3: Battery parameters [71] [75] [72] [76] [73] [74]

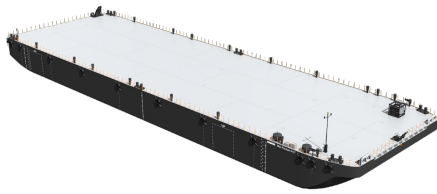
	Lead-acid	Lithium-ion
Energy density [kWh/ m^3]	25-90	94-500
Capital costs [€/kWh]	170-340	200-700
DoD [%]	50-75	90-95
Efficiency [%]	85-90	90-95
Lifetime [cycles]	200-300	500-2000

2.4. FLOATING PLATFORMS

Since the project is offshore, floating platforms are necessary for most of the components to buoy. There are many different types of floating structures available, such as spar, semi-submersible, tension leg platform and others [77]. However, looking at the footprint of the electrolyzer facility, the area needed is in the scale of thousands of square

meters, and therefore, larger structures should be used. For this purpose, a flat deck barge is a great option (figure 2.15). Barges are mostly used for transporting goods, but they can be used for providing buoyancy to offshore equipment as well.

2



(a)



(b)

Figure 2.15: Stan Pontoon 9127, constructed by Damen Shipyards Group [78]

There are several barge sizes available in the market, with 300 ft barge to be the most extensively used. The length of this barge is 91.440 m (300 ft), the moulded breadth of 27.432m (90 ft), the moulded depth of 6.096 m (20 ft), the deadweight of 9700 tons and the deck area is about 2500 m^2 [79].

3

SYSTEM DESIGN

In this chapter, the important parameters regarding the cost and size of the different components will be selected, based on the findings of the literature review. Overall, the lifetime of the project is considered equal to the component with the highest lifetime, the PV panels, and therefore, this would be 20 years. Since, not every component has 20 years of lifetime, some of them might need to be replaced, and thus, a replacement cost should be considered as well.

3.1. FLOATING PV

3.1.1. PV MODULES

In section 2.2.3, the different kinds of PV panels were presented. Rigid panels are selected for the project, due to their higher efficiency. According to Fraunhofer ISE [58], the lab module efficiencies of mono-crystalline panels are up to 24.4 %. Therefore, it can be assumed that in 2030, this could be the actual efficiency of the mono-crystalline panels. The area of the module is considered to be $1 \times 1.65 m^2$, which corresponds to a rated power of 403 W_p . The projections for 2030 estimate that the price of the c-Si modules will be in the range between 0.11-0.19 €/ W_p . Therefore, an average price of 0.15 €/ W_p is chosen for this study [62]. The parameters of the selected PV modules are presented in table 3.1:

Table 3.1: PV module parameters [61] [62] [59] [58] [60]

Area	1×1.65	m^2
P_{module}	403	W_p
Efficiency	24.4	%
Cost	0.15	€/ W_p

3.1.2. BALANCE OF SYSTEM

The main components of a floating PV system were presented in section 2.2. The PV modules, which were just presented in the previous section, are mounted on a floating platform. The platform is kept in the desired place by the anchoring and mooring system. Power electronics are used in order to regulate the voltage and current of the FPV system. Finally, cables are used to transfer the produced power to the electrolyzer.

Floating structures are essential for FPV systems. In chapter 2, the commercially available floating structures for FPV systems were presented. In this research, the membrane proposed by Ocean Sun is selected. This technology is the only available on a commercial level and already tested in sea water environments. In addition, the PV module's operating temperature is decreased due to the direct contact with water, resulting in improved efficiency. Finally, Ocean Sun provides extended information about this patent, in contrast with the other manufacturers, which hide most of the information. Ocean Sun [64] offers a structure, which consists of a thin polymer membrane attached to a floating ring, to provide the required buoyancy to the panels. They offer two different platform sizes, one of 75 m (650 kW_p) and one of 50 m (280 kW_p). The first configuration, includes 1944 crystalline silicon 60-cell modules, while the second one 848 [64]. For the larger platform, this corresponds to PV modules of 334 W_p each. Since, the selected modules for this projects have a rated power of 403 W_p , the whole platform size would be approximately 783 kW_p . As can be noticed in figure 3.1, the modules are placed flat on the membrane, with zero tilt angle. The selected platform can be seen in figure 3.1.

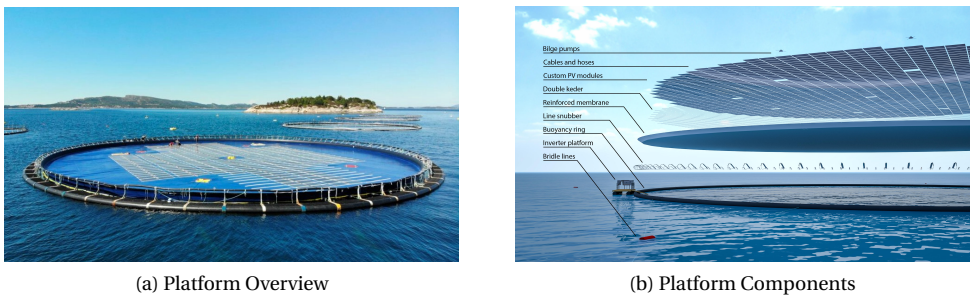


Figure 3.1: Ocean Sun's patented technology [64]

The cost of the balance of system for FPV is a parameter with great uncertainty. Most investors do not usually publish the cost analysis of real projects, making the total cost of a PV system very uncertain. This is even more ambiguous for offshore FPV systems, which are still in a starting level. The prices of the modules are already known, but BoS prices vary depending on the project. The main difference in investment costs between floating PV and ground-mounted PV is in the BoS, including the floating structure, the anchoring and mooring system, the electrical equipment and the offshore installation costs. Since, the technology is at a very early stage, especially for offshore systems, it is very difficult to provide detailed information about the cost analysis of the system. In addition, unique systems should be designed for the different projects, depending also on the location.

Large-scale offshore floating structures are projected to have the same price as land-based structures by 2030 [80]. The structure costs of land-based PV modules are reported to be 0.08 €/W_p, including the anchoring and mooring system [81]. Instead of an inverter, a DC/DC converter is used. For the DC-DC converters, it is assumed that the converter cost depends on the power rating and that DC-DC converter cost learning rates are the same to the inverters' rates. The price of DC/DC converter is reported to be 0.08 €/W_p [59]. However, in utility-scale projects the price of the inverter falls to 0.02 €/W_p [82] and the same is assumed for the DC-DC converters. The installation costs are 0.075 €/W_p [82] for utility-scale land-based installation. Having no information about how this costs would turn out to be in the offshore environment, an assumption was made. The installation costs for offshore utility-scale PV systems are considered to be 20 % higher. Finally, the electrical components of the system, according to the World Bank report [51], cost approximately 0.11 €/W_p. Since, the system modelled in this report is not including grid connection components and transformers, their costs should be decreased [83] [84] and they are assumed to be 0.06 €/W_p. Overall, the BoS costs are calculated to be 0.25 €/W_p.

This result is verified also by Ocean Sun [85] [64]. For this research, the membrane proposed by Ocean Sun will be used, as already presented. After discussions with Ocean Sun, for large scale systems (>50 MW_p), the total CAPEX of the FPV System is 0.45 \$/W_p (0.378 €/W_p). More than half of the cost belongs to the PV modules. However, Ocean Sun installations take place near-shore and in semi-sheltered waters. Therefore, the balance of system costs will be higher for offshore environments. This is due to the higher cables cost, the higher mooring system cost and the higher installation costs. Therefore, the total costs for local offshore installations are reported to be around 0.55 \$/W_p (0.462 €/W_p) [85]. Assuming price drops in both the PV modules and the BoS by 2030, the overall FPV system cost is selected to be 0.4 €/W_p, as can be seen in table 3.2.

Table 3.2: Costs for the OFPV system [61] [62] [59] [60] [84]

PV Module	0.15	€/W _p
Structure	0.08	€/W _p
DC-DC Converter	0.02	€/W _p
Installation	0.09	€/W _p
BOS _{Electrical}	0.06	€/W _p
Total	0.4	€/W_p

3.2. ELECTROLYSER SYSTEM

In section 2.1.2 the different electrolyser technologies were presented in detail. Alkaline and PEM electrolyzers are the only technologies that are commercially mature. Alkaline water electrolyzers have lower cost than PEM, since expensive metals are not required. However, they have lower current density, which means that larger areas are needed to produce the same amount of hydrogen. Therefore, both technologies can be used in this project, and therefore, each choice should be examined.

Normally, the electrolyzer efficiency varies over the operating range of the electrolyser. More specifically, the efficiency is higher for partial load operation [86]. However, for the purpose of this study, the system efficiency is assumed to be constant. The efficiency of alkaline electrolysers is assumed to be 83% for the HHV of hydrogen [42], which corresponds to a specific power consumption for the electrolyzer of 47.6 kWh/kg [33]. The specific electricity consumption of PEM electrolyzers is currently 52 kWh/kg and it is expected to reach 50 kWh/kg by 2030 [87] [32] due to technology development. Therefore, the efficiency of PEM electrolyzers is 78.8 % for the HHV of hydrogen.

The footprint of the electrolyzer is a very important parameter, especially for offshore systems. An electrolyzer facility, apart from the electrolyzer units, includes the water treatment facility, the electrical equipment, the compression units and the control rooms and offices [28]. Assuming that converting a plant like that to offshore, means a more compact design, less area is needed. In addition, since no conversion to DC is needed, a significant portion of the footprint suggested in the literature can be neglected. Finally, improvements on technology can also help reduce the plant footprint. Therefore, considering 25 % decreased size and taking conservative values from the literature ($0.095 \text{ m}^2/\text{kW}$ for alkaline and $0.048 \text{ m}^2/\text{kW}$ for PEM), the footprint of alkaline is considered equal to $0.07 \text{ m}^2/\text{kW}$ for alkaline electrolyzers and $0.035 \text{ m}^2/\text{kW}$ for PEM.

Given the fact that, in this research, the project is based on hourly data and the fact that the cold start-up time takes place once per day, for a low irradiance period, the start-up time is neglected. The same is considered for the ramp-up and down times of the electrolyzer.

The lifetime of the electrolyzer is different for the stack and the rest of the plant. The latter has a lifetime of 30 years while stacks have lifetime of about 60,000 to 90,000 hours [19]. Since the lifetime of our project is considered 20 years, the stack replacement will take place one time. The stack replacement cost is considered to be 30% of the investment costs, assuming further price drops in the following decade [88] [89].

The electrolyzers, are usually split into multiple stacks in parallel and therefore, the fixed and unscheduled maintenance periods are expected to be low. The availability of electrolyzers is reduced due to planned and unplanned maintenance. This value is reported to be 8,585 hours, which means that 175 hours of the year the electrolyzer will be shut down for maintenance [33]. This is also confirmed by [90], which indicates that the planned maintenance is 5 days per year, split into 2 events, while the unscheduled maintenance is expected to occur 4 times per year, with a duration of 14 hours.

The projections for Alkaline electrolyzer costs for multi-MW scale, are around 400 €/kW [91] [92] and 500 €/kW for PEM [36] [34] by 2030. However, according to McKinsey & Company report for Hydrogen Council [21], states that the learning rates could be much higher, especially if compared to the ones of solar PV and batteries. This could decrease the electrolyzer CAPEX even more to 200 and 300 €/kW for Alkaline and PEM respectively. The operation & maintenance cost, for large scale electrolyzers is estimated to be 1.52% [33], with this value expected to drop further to 1% by 2030.

All the electrolyzer parameters selected can be summarized in table 3.3:

Table 3.3: Electrolyzer parameters [42] [29] [42] [32]

Parameter	Alkaline	PEM	%
Efficiency (HHV)	83	78.8	%
Pressure _{out}	30	30	bar
Electricity Consumption	47.6	50	kWh/kg
Stack Lifetime	78,000	78,000	hours
Footprint	0.075	0.035	m ² /kW
Weight	0.03	0.01	kg/W
Capex	200	300	€/kW
O&M Cost	1	1	% Capex/year

3.3. OTHER COMPONENTS

3.3.1. BATTERY

In section 2.3, the possible battery types to use in the system were compared. Lithium-ion batteries are selected due to their higher energy density and longer life cycle. The main problem of lithium-ion batteries is related to their cost, as they are very expensive at the moment. However, their costs are projected to decline in the future. The depth of discharge (DoD) for lithium ion batteries is reported to be 90% [74]. The round trip efficiency of lithium-ion batteries is 95 %. The lifetime of lithium ion batteries is expected to be around 4,000 cycles or 10 years by 2030 [73] [74]. Assuming one cycle per day, this means that the batteries need to be replaced once over the lifetime of the project. The battery investment cost after 10 years is expected to drop by 20%, therefore the battery replacement cost is chosen to be 80% of the capital cost. The battery parameters are presented in table 3.4:

Table 3.4: Battery parameters [72] [76] [73] [74]

Rated Power	10	kWh
Round Trip Efficiency	95	%
Depth of Discharge	90	%
Investment Cost	100	€/kWh
O&M Cost	1	% Capex/year

The price of batteries is declining over the years, and it is expected to decline even more until 2030. Currently the battery costs are around 200 €/kWh. However, there are projections that the cost of lithium-ion batteries for stationary applications to be around 100 €/kWh, for MW scale applications [70] [93]. According to Bloomberg New Energy Finance (BNEF), lithium-ion battery pack prices are expected to be close to 100 €/kWh by 2023 and drop even further to 40 €/kWh by 2030 [72]. However, this is a very optimistic consideration. The operation and maintenance cost of the battery system is considered 1% of the investment cost of the battery [76].

3.3.2. COMPRESSOR

In order for hydrogen to be injected to the central network, a higher pressure of 100 bar is needed. The output pressure of the water electrolysis is considered to be 30 bars, and therefore, a compressor is needed. To size the compressor, the rated production of hydrogen is taken into account. The compressor is assumed to be a single stage mechanical compressor for simplicity. The capital cost of the compressor is assumed to be 2500 €/kW [94] and the operation and maintenance cost is considered to be 4% [42]. The energy consumption of the compressor is calculated from equation 4.11, presented in chapter 4. The lifetime of the compressor is 15 and therefore, it needs to be replaced once during the lifetime of the project. A replacement cost factor of 100 % is considered in the calculations. The compressor parameters can be seen in table 3.5:

Table 3.5: Compressor parameters [94] [42]

Investment Cost	2500	€/kW
O&M Cost	4	% Capex/year
Lifetime	15	years

Overall, all the components of the proposed hydrogen system are presented, along with the main sizing and cost figures. In the next chapter, and in order to identify the final size and dimensions of the system, a model needs to be designed and simulated based on the numbers presented in this chapter.

4

SYSTEM MODELING

This chapter presents the modeling approach of the proposed solar-to-hydrogen system. The components are modelled using MATLAB 2020b and Simulink software. The model validation and verification can be found in Appendix A.

4.1. OVERVIEW OF SYSTEM CONFIGURATIONS

An overview of the hydrogen production system was presented in chapter 1. As mentioned in chapter 1, in the proposed systems, two parameters should be examined. The first one is the electrolyzer technology, since both alkaline and PEM could fit in this project. The second parameter is the potential use of batteries in the system, in order to keep the electrolyzers operating during the night. Batteries increase the energy usage of the hydrogen production system, by storing the excess energy during the day and using it to power the electrolyzers during the night. However, their cost is a major obstacle. In total, 4 different systems need to be modelled (as shown in table 4.1). Two system configurations are based on alkaline electrolyzers, and two on PEM electrolyzers. For each electrolyzer technology, two systems are modelled, one including batteries, and one not.

Table 4.1: System Configurations

	Electrolyzer Technology	Battery Included
1	Alkaline	No
2	Alkaline	Yes
3	PEM	No
4	PEM	Yes

In order to calculate the system dimensions and cost, a control strategy should be implemented for each system. The control strategy decides how to use the energy production of the OFPV system. When batteries are not included, the control strategy is

simpler, while in the other case it is more complicated. In terms of electrolyzer technology, the only difference in the control strategy is the minimum operating level of each technology. More specifically, alkaline electrolyzers cannot operate below 10% of their maximum load, while for PEM electrolyzers, this level is considered 1%. In practice, electrolyzers are usually split into multiple stacks in parallel. For this research, we assume that the stacks have 5 MW rated capacity each. This is assumed on the basis of the maximum nominal power per stack available on the market [19] [87]. Therefore, if the input power is below 0.5 MW (for alkaline), the electrolyzer shuts down completely. If the power is above 0.5 MW, the electrolyzer power can be varied by switching off stacks. In the following paragraphs, more details on the control strategy of each system configurations will be elaborated.

4

4.1.1. CONFIGURATIONS WITHOUT BATTERIES

In this configurations, the electrolyzer is connected with the OFPV system, without the use of any temporary storage. Power electronics are used to regulate the current and voltage to the operating level of the electrolyzer. More specifically, a direct current (DC-DC) power converter and a maximum power point tracker (MPPT) are connected between the electrolyzer and the PV modules. The main impact of the MPPT is to harvest the maximum possible energy, while the DC-DC converter adjusts the current and voltage from the PV modules to the electrolyzer. The electrolyzer is split into stacks, in parallel, making it is possible to change the power consumption of the overall system by switching off individual electrolyzers. Therefore, the electrolyzer system minimum partial load will be 10% of the single stack's capacity. Below this point, there is no hydrogen production.

The electricity for the reverse osmosis unit and compressor unit is provided from the FPV system. It should be mentioned that a small number of batteries is needed for providing power to the control systems, in order to turn on and off the electrolyzer when there is not enough power provided. The power needed to be provided by the battery system is modelled as 0.01 % of the rated capacity of the electrolyzer. From this moment, to avoid confusion between the different system configurations, this configurations will be referred as configurations without batteries, even though a small amount of batteries will be used. The configurations without the use of battery, can be seen in figure 4.1:

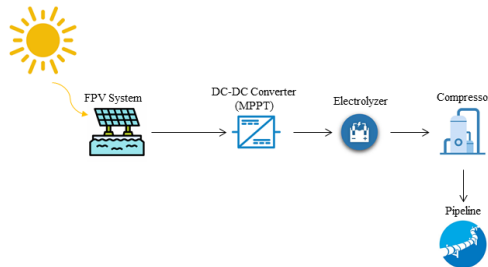


Figure 4.1: Overview of the system configuration without the use of battery system

The control strategy for the configurations without the use of battery is simple, and

can be seen in figure 4.2. To begin with, the model reads the meteorological data, the PV array data and the electrolyzer data. In the next step, the output power of the FPV system is calculated. If the power output of the FPV system is higher than the maximum capacity of all electrolyzer stacks, the excess power is dumped. The same happens also in the case where the output power of the FPV system is lower than the minimum capacity of a single stack. If the output power of the FPV system is between the maximum and the minimum electrolyzer capacity, the electrolyzer uses the necessary amount of stacks and the model calculates the amount of produced hydrogen. At this point, it is worth highlighting that the model and the research in general, does not take into account how the power output of the OFPV system is split in the electrolyzer stacks.

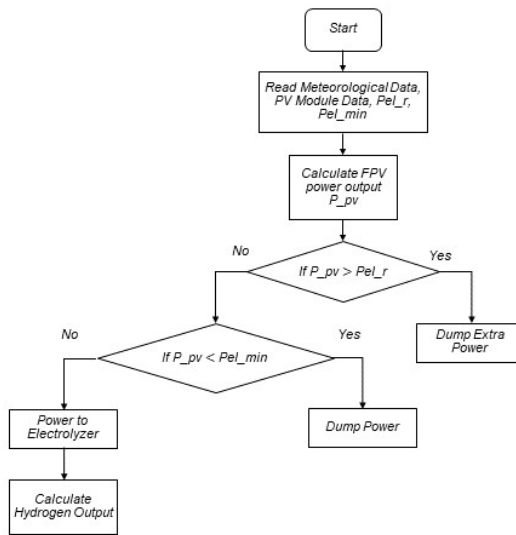


Figure 4.2: Flow chart of the control logic for the configurations without batteries

Regarding the sizing of the system, the electrolyzer capacity is sized to meet the OFPV system capacity and therefore has the rated capacity of the OFPV system, minus the power needed by the compressor, the batteries used for the control system and the reverse osmosis plant. The sizing of the system is performed under the target of producing 1 million tons of hydrogen per year. Taking the alkaline electrolyzer case as an example, it can be seen in figure 4.3, that by decreasing the electrolyzer capacity and keeping the FPV system capacity at the same levels, the levelized cost of hydrogen (LCOH) decreases. In practice, this means that excess energy is dumped from the system, since no temporary storage is included. Therefore, in terms of costs, it is preferred to waste some of the produced energy.

The Simulink model of the overall system of the configurations without batteries,

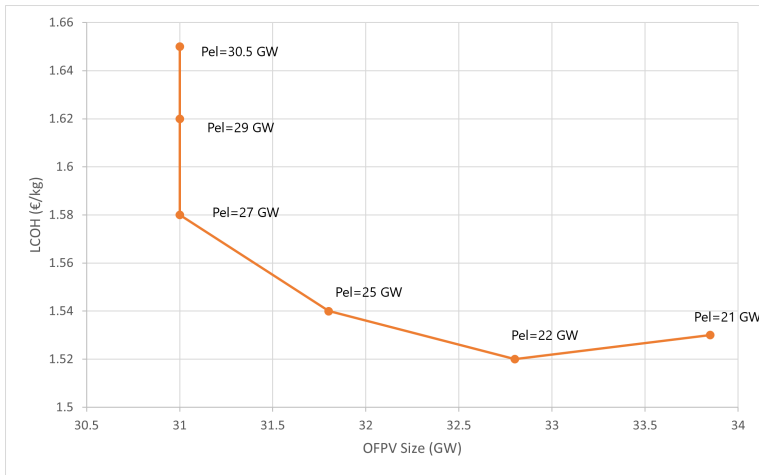


Figure 4.3: Sizing methodology for the OFPV and electrolyzer capacities

depicted in figure 4.4.

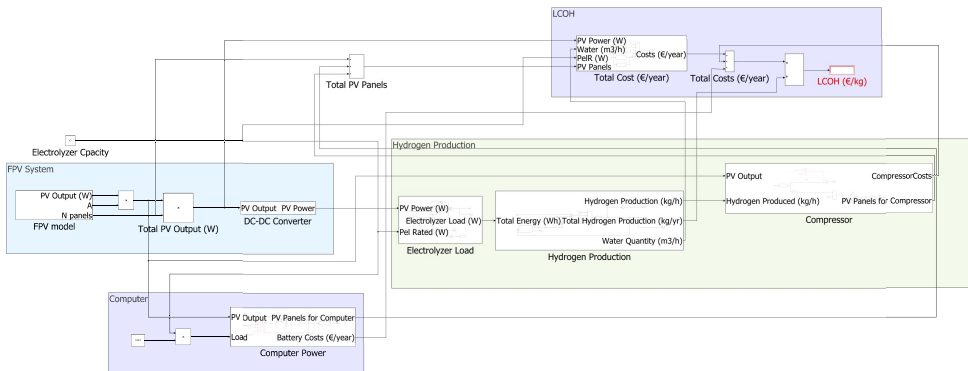


Figure 4.4: Total system without batteries, modelled in Simulink

4.1.2. CONFIGURATIONS WITH BATTERIES

In practice, it is preferred to run electrolyzers at a constant load, to ensure longer lifetime. Electrolyzers, as mentioned in chapter 2, require some time to turn on/off and to increase/decrease their level of operation. Therefore, by keeping the electrolyzers open at all times, this problem is eliminated. Batteries could potentially keep the electrolyzers operating at a constant capacity all the time. In this configurations, batteries are added and operate as an instantaneous and daily energy buffer for storing the fluctuating power output of the FPV system. The target of the battery involvement in the system,

is to stabilize the input load of the electrolyzer and use the excess power to keep the electrolyzers operating during the night. The power for the reverse osmosis facility and the compressor facility is provided from both the FPV system and the batteries. A schematic representation of the configurations including batteries, can be seen in figure 4.5:

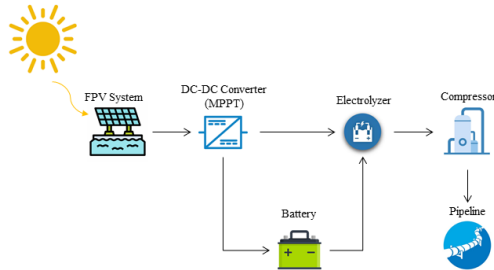


Figure 4.5: Overview of the system configuration using batteries

Ideally, by using batteries, the electrolyzers could operate at the rated capacity all the time. However, for a large-scale system this would require an excessive amount of batteries and would lead to a significantly higher cost. Therefore, the battery involvement will be investigated only in terms of operating the electrolyzer at a stable load and at the minimum capacity, at low irradiance levels. For this reason, different operating levels for the electrolyzer should be determined. Five different operating points of the electrolyzer are selected. It should be highlighted here, that since the target is to keep the electrolyzer system open at all times, each stack should operate at least at the minimum capacity and switching on and off stacks to vary the power input is not an option for this configurations. The lowest possible operating point depends on the technology used. More specifically, it is 10% of the rated capacity for the alkaline electrolyzer and 1% for PEM. Therefore, the levels for the configuration based on alkaline technology are 10%, 25%, 50%, 75% and 100% and for the PEM case the levels are 1%, 25%, 50%, 75% and 100%. The electrolyzer load is defined by the output of the FPV system. When the OFPV output power is higher than the electrolyzer rated power, the electrolyzer operates at its maximum capacity. When the OFPV output power takes values between 75 and 100% of the electrolyzer rated power, then the electrolyzer operates at 75% of its rated capacity. When the OFPV system generates power between 50 and 75% of the electrolyzer peak power, the electrolyzer runs at 50% of its capacity. In the same direction, in the case the OFPV power output takes values between 25 and 50% of the rated power, the electrolyzer operates at 25% of the rated capacity. Finally, when the OFPV power is less that 25% of the electrolyzer capacity, the model checks the battery state of charge. If the battery is charged at least by 50 % then the electrolyzer operates at its full load, while in the other case, the electrolyzer operates at its minimum load. The electrolyzer load formation can be summarized in figure 4.6 for the alkaline case. For the PEM case, instead of 10 % minimum load, this value is 1%.

At this point, a control strategy should designed and implemented, deciding the mo-

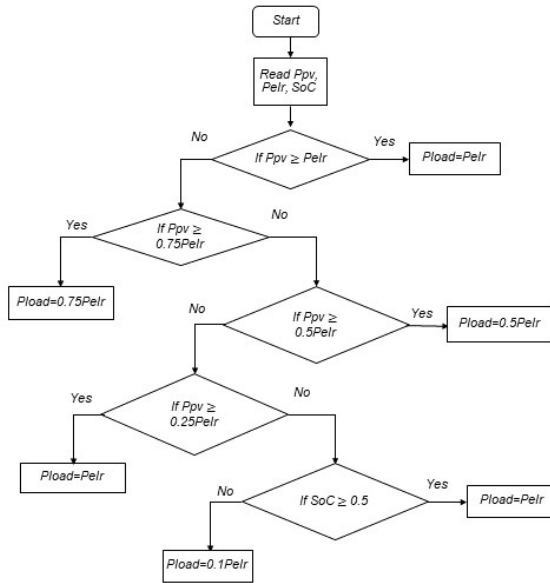


Figure 4.6: Electrolyzer load depending on the output of the FPV system, for the alkaline case.

ments the energy produced should be stored in the battery or consumed by the electrolyzer. The control strategy is depicted in figure 4.7:

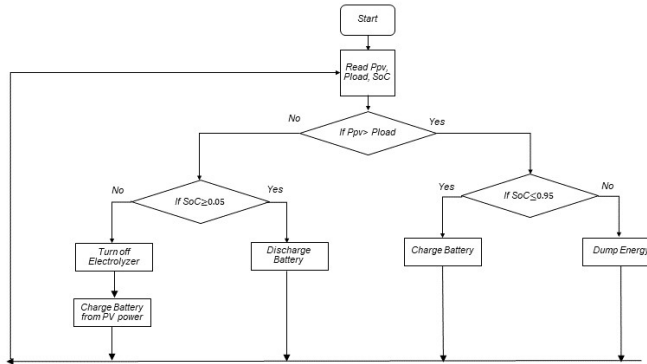


Figure 4.7: Flow chart of the control logic of the battery

In this system configurations, energy surplus is possible to happen when the electrolyzer cannot import more power, and the battery cannot store more energy. In addition, energy deficit may happen, when the FPV output is less than the minimum electrolyzer load and the battery cannot provide more power. The main reason for the deficit

and surplus is the different irradiance levels between winter and summer. A solution to this problem could be oversizing the PV and the battery systems. However, something like that would increase the costs significantly. The control logic of the battery system, modelled in Simulink can be seen in figure 4.8:

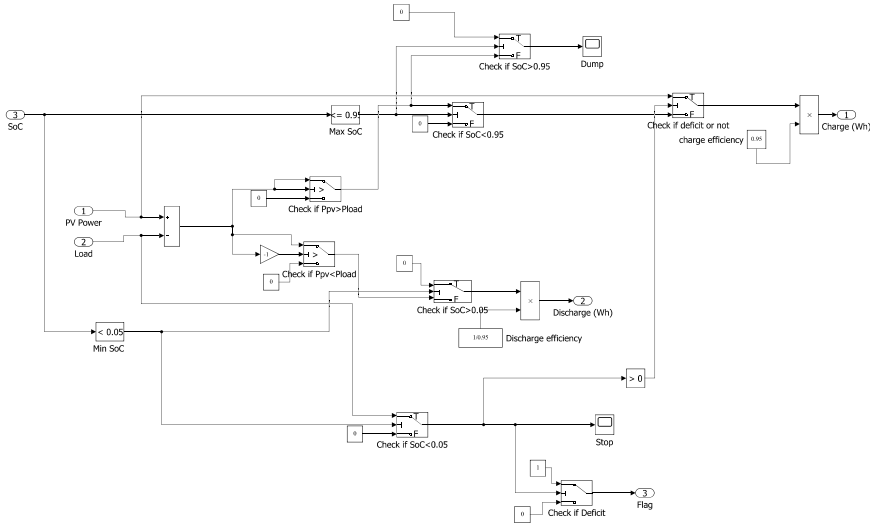


Figure 4.8: Battery control strategy model in Simulink

The sizing strategy is the same as presented in section 4.1.1, aiming for the minimum LCOH. The Simulink model of the configurations including batteries is depicted in figure 4.9:

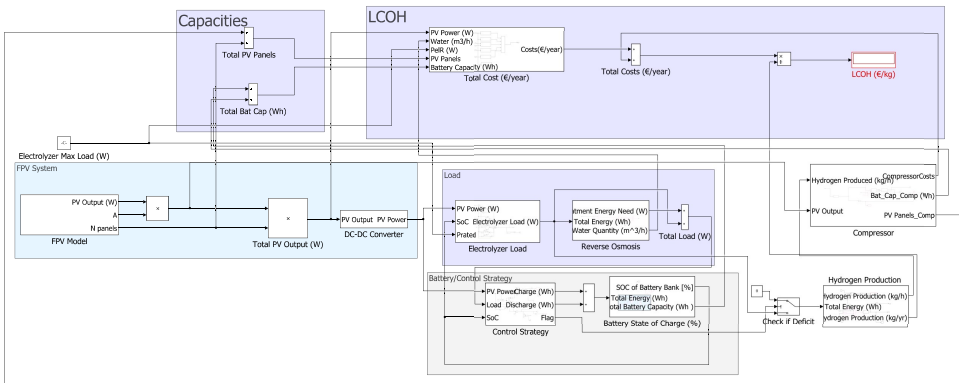


Figure 4.9: Total system with batteries model in Simulink

4.2. COMPONENT MODELLING

After the overall model was presented, the specific model of each component will be elaborated.

4.2.1. FPV SYSTEM

For the modelling of the FPV system, meteorological data from the Photovoltaic Geographical Information System (PVGIS) database for a typical meteorological year were used. This data were used as input for the Simulink model. The power output of PV is calculated from the simple efficiency model [48] [95]:

$$P_{PV} = N_m \times A_m \times G \times \eta_m \quad (4.1)$$

Where N_m is the number of modules, A_m is the rated capacity of the module, G is the total irradiance on the module, and η_m is the efficiency of the module. As described earlier, the PV modules are placed flat on the membrane, and therefore, the total irradiance is equal the global horizontal irradiance (GHI) on the module. The efficiency of the module, η_m , is calculated, taking into account the temperature correction model [48] [95]:

$$\eta_m = \eta_{mSTC} \times [1 + k \times (T_m - T_{STC})] \quad (4.2)$$

Where T_{STC} is the PV cell temperature under STC ($25^\circ C$), k is the temperature coefficient of power (for crystalline silicon modules, k is $-0.0035 / ^\circ C$ [48]) and η_{mstc} is the module efficiency at STC. Normally, the module efficiency is also depended on the irradiance level. However the effect of irradiance on the module efficiency will be neglected on this research for simplicity, and this value will be considered constant and equal to the PV efficiency given by PV manufacturers. Therefore, only the influence of the temperature will be taken into account, as shown in equation 4.2. Several models have been proposed for calculating the temperature of land-based PV modules. For the floating PV case, there are some suggestions in the literature, such as the models proposed by [96] and [97]. In this thesis, the model proposed by [97] will be used. The module temperature is therefore, calculated from:

$$T_m = 0.943 \times T_W + 0.0195 \times G - 1.528 \times V_{wSea} + 0.3529 \quad (4.3)$$

Where $T_W = 5.0 + 0.75T_a$ is the sea temperature, T_a the ambient temperature, $V_{wSea} = 1.62 + 1.17 \times (V_{WLand})$ and V_{WLand} is the land wind speed. T_a and V_{WLand} data are imported from Photovoltaic Geographical Information System (PVGIS) database [16]. The two equations just presented were proposed in [97] and they are used to relate land and sea level values, since from PV GIS database only data about land are available. The average air temperature based on the data used in this thesis is calculated $19.18^\circ C$, and this is validated from the Global Solar Atlas database, which provides almost the same value ($19.2^\circ C$) for the specific location.

An important parameter that should be taken into account in the PV system analysis is the degradation rate of the PV panels. According to the literature, 0.5% per year is the average value and will be considered in this research [60]. The energy output used in the LCOE calculations is affected from the degradation rate, according to the following equation [98]:

$$E_f = E \times (1 - DR)^n \quad (4.4)$$

Where E_f is the energy output of the PV system, E the energy output of the first year, without considering degradation, DR is the degradation rate and n is the lifetime of the project.

Another important parameter is losses. There are several types of losses that should be considered. OFPV systems face rough environmental conditions, which lead to continuous movement. This movement results in different irradiance levels on the modules on the same string, generating different voltage and current values across connected modules [63]. Given the lack of data in the literature, about how much is the PV output affected by this movement, this kind of losses are neglected in this research. In addition, soiling is also a very significant loss mechanism in OFPV systems. Soiling includes different types of dirt on the surface of the module, such as salt stains, dust or bird droppings, leading to partial shading of the modules [63]. These losses are considered to be 1%. Finally, the cabling losses are considered to be the same to a typical land-based PV system, 1% [99].

An overview of the FPV model can be seen in figure 4.10:

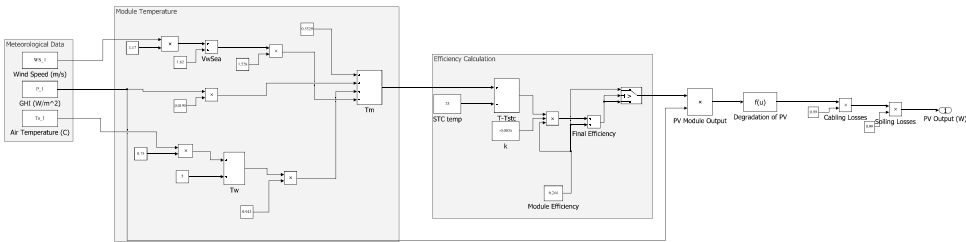


Figure 4.10: Overview of the floating PV model in Simulink

DC-DC CONVERTER

A DC-DC converter is a device that changes the input voltage and current to different levels [56]. The power output of the DC-DC converter, due to losses, differs slightly from the power input and can be calculated from:

$$P_{el} = P_{PV} \eta_{DC-DC} \quad (4.5)$$

Where, P_{el} (W) is the power input of the electrolyzer, P_{PV} (W) is the power output of the FPV module and η_{DC-DC} is the efficiency of the DC-DC converter, which in our case, is assumed to be 99 % [59].

For each different system configuration, the total energy produced from the FPV system, including the losses, is presented in table 4.2:

4.2.2. ELECTROLYZER MODEL

The performance of electrolyzers depends on many factors, such as voltage, current, pressure, temperature, electrode spacing, and electrolyte concentration. However, these

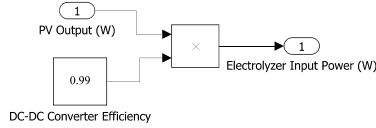


Figure 4.11: Overview of the DC-DC converter model in Simulink

Table 4.2: Energy produced from the FPV system

	Alk/No Bat	Alk/Bat	PEM/No Bat	PEM/Bat	TWh
E_{PV}	53	54	59	60	

4

factors will not be examined in this report, as the main target is to design and evaluate the system as a whole and not to investigate specifically the fundamentals of water electrolysis technologies. To calculate the hydrogen produced from the electrolyzer m_{H_2} (kg/h), the following equation is used [100]:

$$m_{H_2} = \frac{\eta_{el} \times P_e}{E_{HHV}} \quad (4.6)$$

Where η_{el} is the efficiency of the electrolyzer, P_e (W) is the input load of the electrolyzer and E_{HHV} is the high heating value of hydrogen (Wh/kg).

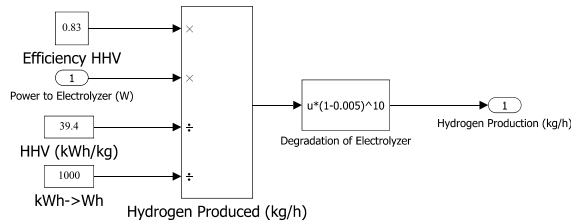


Figure 4.12: Overview of the electrolyzer model in Simulink

As mentioned above for the PV panels, electrolyzers also degrade over time. The degradation rates reported in the literature are usually for continuous usage. It is not clearly reported, what is the effect of the variable input power operation to the degradation of electrolyzers. Degradation causes the specific energy consumption to increase to produce hydrogen. The degradation rate of electrolyzers is assumed to be 0.54% per year, according to [101]. The hydrogen output is affected from the degradation rate, according to the following equation:

$$m_{H_2f} = m_{H_2} \times (1 - DR)^n \quad (4.7)$$

4.2.3. BATTERIES

The state of charge of the batteries can now be calculated in the following way:

$$SoC = \frac{E_b}{E_{b_{total}}} \tag{4.8}$$

Where, E_b is the battery capacity at every moment, and $E_{b_{total}}$ is the total battery capacity:

$$E_{b_{total}} = C \times DoD \times N \tag{4.9}$$

where C is the capacity of the battery (Wh), N is the number of batteries in the system and DoD is the depth of discharge of the battery. The Depth of Discharge is defined as:

$$DoD = SoC_{max} - SoC_{min} \tag{4.10}$$

with SoC_{max} the upper limit on the SoC, 0.95 in our case, and SoC_{min} the lower limit on the SoC, 0.05 for our system.

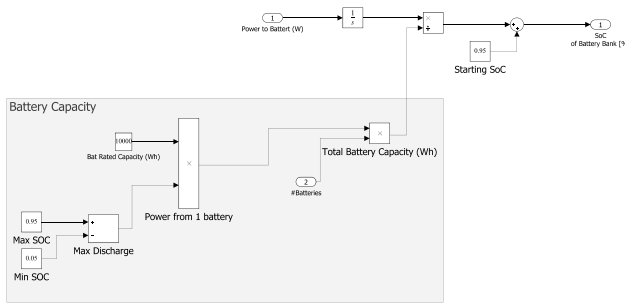


Figure 4.13: Overview of the battery model in Simulink

For simplicity, parameters such as the self-discharge rate and degradation rate of the battery are neglected from this research. For each different system configuration, the battery capacity needed is calculated as in table 4.3:

Table 4.3: Battery Capacity for the different system configurations

	Alk/No Bat	Alk/Bat	PEM/No Bat	PEM/Bat	
Battery Capacity	4.4	52.7	4.4	40.2	GWh

4.2.4. COMPRESSOR MODEL

The energy consumption of the compressor can be calculated by [102] [103]:

$$E_{comp} = \frac{T \times R \times Z \times r}{\eta_{mcomp} \times M \times \eta_{is} \times (r - 1)} \left(\frac{p_2}{p_1} \frac{r-1}{r} - 1 \right) \tag{4.11}$$

Where Z ($=1.04$) is the compressibility factor for H_2 , R is the universal gas constant ($8.3145 \text{ J/mol} \times K$), T is the temperature of hydrogen when entering the compressor (293

K), P_1 and P_2 are the compressor's pressures (30 bar input and 100 bar output), r is the ratio of specific heats of hydrogen (1.41), M is the molecular mass of H_2 ($=2.02$ g/mol), η_{mcomp} is the mechanical efficiency (98%) of the compressor and η_{is} is the isentropic efficiency of the compressor ($=0.8$). The required rated capacity of the compressor is calculated by:

$$P_{comp} = E_{comp} \times \dot{m} \quad (4.12)$$

Where \dot{m} is the hydrogen mass flow rate through the compressor (kg/s). The model for calculating the capacity of the compressor is depicted in figure 4.14.

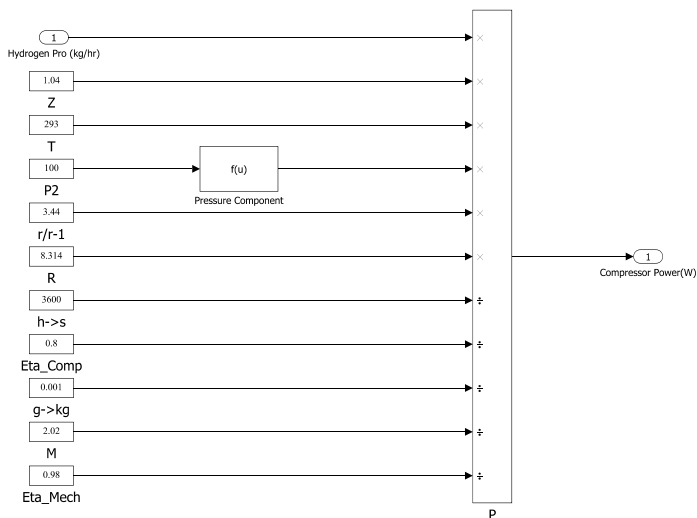


Figure 4.14: Overview of the compressor subsystem in Simulink

The compressor capacity for each different system configuration, is calculated as in table 4.4:

Table 4.4: Compressor Capacity for the different configurations

	Alk/No Bat	Alk/Bat	PEM/No Bat	PEM/Bat	
Compressor Capacity	277	239	263	262	MW

4.2.5. PIPELINES

The pipelines are used to transfer the generated hydrogen from the compressor to the pipeline network. In order to calculate the cost of the pipelines, their diameter D (m) should be calculated [42]:

$$D = 2 \times \sqrt{\frac{P}{\pi \times v_{H_2} \times \rho \times E_{HHV} \times 3.6}} \quad (4.13)$$

The density of hydrogen $\rho(kg/m^3)$ at 100 bar pressure and 293 K temperature, is $8 kg/m^3$ [104]. The velocity of hydrogen $v_{H_2}(m/s)$ is considered 30 m/s [105]. The high heating value of hydrogen $E_{HHV}(kWh/kg)$ is 39.4 (kWh/kg). P(MW) is the capacity needed from the pipeline, calculated based on the efficiency of the electrolyzer. The life-time of the pipelines are 40 years [105]. Although pressure drops along the pipeline are sensitive to the distance travelled and the flow rate of the fluid, this was not accounted for, for simplicity.

The investment costs of the pipeline are calculated based on the discretization investment costs of natural gas pipelines [42] [106]:

$$Capex_{pip} = 278.24 \times e^{1.6 \times D} \quad (4.14)$$

In this equation, extra 5% costs should be added for the conversion from natural gas to hydrogen pipelines. However, since the pipelines will be new in this project, the extra percentage will not be added. In addition, the operation and maintenance costs are considered to be 1% of the capital costs.

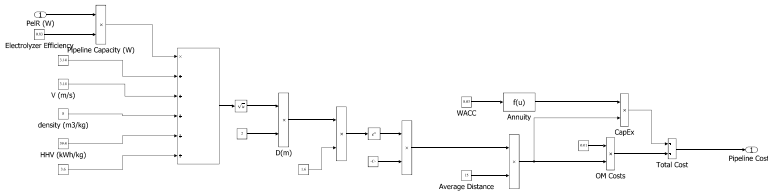


Figure 4.15: Overview of the pipeline cost calculation in Simulink

The pipeline diameter for each different system configuration, is calculated as in table 4.5:

Table 4.5: Pipeline properties for the different configurations

	Alk/No Bat	Alk/Bat	PEM/No Bat	PEM/Bat	
Diameter	0.83	0.77	0.83	0.83	m
Cost	1044	952	1044	1044	€/m

4.2.6. LEVELIZED COST OF HYDROGEN

In order to evaluate the economic feasibility of a hydrogen production system, levelized cost of hydrogen (LCOH) should be calculated. LCOH represents how much a kilogram of hydrogen would cost to be produced. LCOH (€/kg) can be calculated from the following equation:

$$LCOH = \frac{\sum_{i=1}^n CAPEX_i \times annuity_i + OPEX_i}{H} \quad (4.15)$$

Where $CAPEX_i$ is the capital expenditure of each component (€) and OPEX is the annual operational expenditure of each component (€/year). The annualized CAPEX is calculated from the annuity factor, which is calculated from:

$$annuity = WACC \times \frac{(1 + WACC)^{t_i}}{(1 + WACC)^{t_i} - 1} \quad (4.16)$$

Where WACC is the weighted average cost of capital and t_i the lifetime of the component. The WACC used in this research is 3%. WACC is based on the market development of the components of the proposed hydrogen project. Usually, in technologies with low maturity the WACC rates are 5% or 8%. However, most of the technologies used in this project are already mature. More specifically, PV systems are active and mature for the last 20 years. Electrolyzers are also mature and available commercially on a large scale. The same can be said about reverse osmosis facilities, batteries and compressors. The only part of the system that still is at a niche level in the market is the floating structures, which are currently hardly available commercially and on a large scale. However, development is expected in this market, with projects announced on a regular basis and a continuously growing project pipeline. Taking into account also the background knowledge from the offshore industry, it is assumed that in 10 years floating structures for offshore PV projects will be commercially mature. Therefore, the WACC value considered is 3%.

All the cost factors are converted into €, with a conversion rate of 0.82 €/\$. The overall model that calculates the LCOH of the system in Simulink is depicted in figure 4.16:

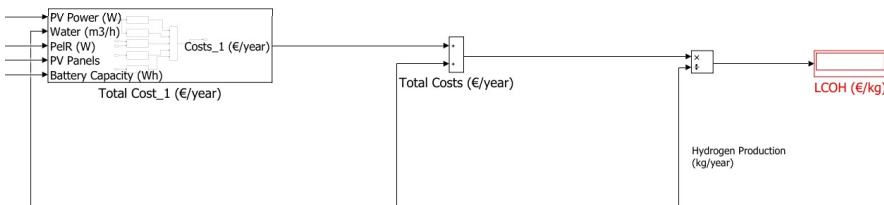


Figure 4.16: Overview of the LCOH model in Simulink

5

RESULTS

This chapter presents the simulation results for the different configurations of the proposed hydrogen system. The final system is selected, in terms of cost and the artist's impression of the system is introduced. Finally, sensitivity analysis is performed, modifying the different input variables to see the response of the output variables.

5.1. CONFIGURATION COMPARISON

As already presented, four different configurations were examined in this research. Simulations of the models presented in chapter 4 were executed based on the input data presented in chapters 3 and 4. The detailed results, including graphs of all the configurations are presented in Appendix B. The sizing and cost results of this analysis are presented in table 5.1.

Table 5.1: Results of the simulation for the four different configurations

	Alk/No Bat	Alk/Bat	PEM/No Bat	PEM/Bat	
PV system	32.6	33.5	37.3	36.9	GW
Electrolyzer	22.0	19.0	22.0	22.0	GW
Batteries	4.4	52.7	4.4	40.2	GWh
Pipeline	18.3	15.8	17.3	17.3	GW
H ₂ Prod	1.03	1.03	1.02	1.02	m ton/yr
Capacity Factor	24.6	28.5	25.9	25.9	%
LCOH	1.5	2.0	1.8	2.2	€/kg

Overall, the most cost-effective solution is the one based on alkaline technology without the use of batteries. Adding batteries to the system, may be more optimal in terms of

energy usage and electrolyzer safe operation, but it also increases the system costs significantly. It is also worth commenting that the use of PEM electrolyzers is also increasing the LCOH, since they are more expensive and less efficient than alkaline.

5.2. FINAL SYSTEM OVERVIEW

Therefore, the final system selected, will be based on alkaline electrolysis. The power produced from the FPV system, is used for covering the load requirements of the electrolyzer, the reverse osmosis plant and the compressor facility. Batteries will only be used for power control systems.

5.2.1. SIZING RESULTS

All the details of the final system are presented in appendix B. Since no batteries are used for energy buffering during the night or during low irradiance hours, the electrolyzer will shut down at this times. Therefore, the maintenance period is assumed to be programmed during the hours that the electrolyzer is not operating and will be neglected in this research. The same happens with start/stop times and ramping up/down losses. Since, in this research hourly data are used, and the times mentioned are in terms of minutes/seconds, they will be neglected as well. The hydrogen production is depicted in figure 5.1.

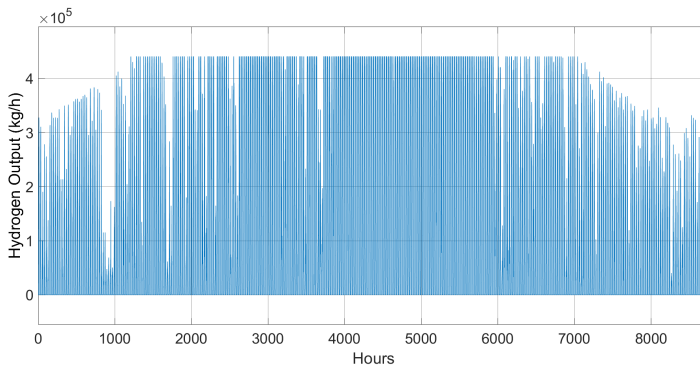


Figure 5.1: Hydrogen Production in the alkaline system configuration with no battery addition

The hydrogen output follows the irradiance form, restricted by the operating limits of the electrolyzer. As can be seen, during the winter period, depicted in the lowest and highest values of the horizontal axis, the hydrogen output is lower, due to the lower irradiance levels. On the other hand, during the summer hours, depicted in the middle of the horizontal axis, the hydrogen production is higher. For this hydrogen production, 32.6 GW of PV capacity are needed, to power 22 GW of alkaline electrolysis. The overall size of the selected system, is presented in table 5.2.

From table 5.2 above, a first impression about the system size is given. It can be easily understood, that in practice, a multi-GW scale system cannot be installed as one unit, and therefore, it should be split to subsystems of smaller size. Current industrial green hydrogen projects do not exceed 20 MW, but 1 GW scale is the target for the industry in

Table 5.2: Selected System Information

	Capacity	Average Daily Amount	Area
FPV System	32.6 GW	153.9 GWh/day	133.7 km ²
Electrolyzer	22 GW	2.8 kt/day	1.54 km ²
Reverse osmosis	0.008 GW	25388 m ³ /day	-
Batteries	4.4 GWh	-	-
Compressor	0.28 GW	2.8 kt/day	-
Pipeline	18.26 GW	2.8 kt/day	-
LCOE (FPV)	0.019 €/kWh	-	-
Investment Cost	21.74 × 10 ⁹ €	-	-
LCOH	1.5 €/kg	-	-

terms of transition from MW to GW scale [28]. Therefore, in this research, the system will be split into subsystems on the basis of 1 GW electrolysis facilities. So, 22 sub-systems are needed. Since the overall system is split into sub-systems, connecting pipelines are also needed, in order to transfer the compressed hydrogen from each electrolyzer facility to the main pipeline, which in turn, will lead hydrogen to the pipeline network. Following the methodology presented in section 4.2.5, each connecting pipeline has a diameter of 0.18 m and a cost of 369 €/m. Therefore, each sub-system will have the following specifications:

Table 5.3: Subsystem Size

Size	Capacity	
PV system	1.48	GW
Electrolyzer	1	GW
Reverse osmosis	0.0004	GW
Batteries	0.2	GWh
Compressor	0.013	GW
Connecting Pipelines	0.83	GW

5.2.2. ARTIST'S IMPRESSION

Overall, the system will be split into 22 subsystems. Each subsystem consists of 2,056 Ocean Sun platforms and 2 floating barges, providing buoyancy to the electrolyzer facility, the compressors, the reverse osmosis plant and the batteries. The number of barges is calculated based on the information provided in chapter 2 and the results presented in table 5.3. More specifically, since a footprint of 75,000 m², with a weight of at least 30,000 t, typical 400 ft barges are selected. A typical 400 ft barge has a deck area of 4500 m² and can buoy up to 20,000 t. Therefore, 2 barges will be used per subsystem, each

one of which consist of 8-9 floors. Therefore, these values will be used, since no detailed studies have been published on offshore hydrogen platforms design and construction. The uncertainty around this issue will be examined through sensitivity analysis. When designing a system, several aspects should be taken into account, such as safety or maintenance. For safety reasons, mooring and anchoring of the FPV system requires some extra space between the platforms. In addition, since the project is offshore, pathways for maintenance boats should be considered as well. Therefore the subsystems, need to be split to more flexible configurations. To create the maintenance pathways, each subsystem is formed as a hexagon, which consists of Ocean Sun platforms formed also in hexagons for the same reasons. In the middle of each subsystems the floating barges are placed. Each subsystem layout can be seen in figure:

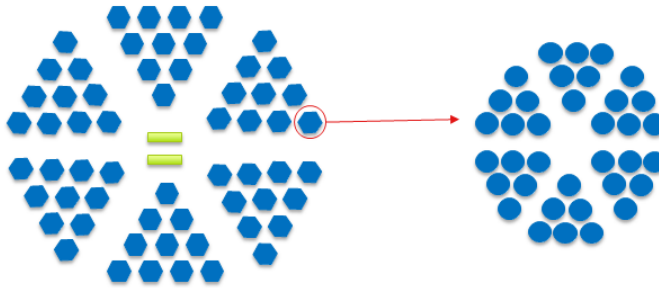


Figure 5.2: Total Subsystem Layout

Between the Ocean Sun platforms, a distance of 10 m is left for safety purposes, and the same happens between the hexagons of platforms. The width of the main maintenance pathways of each hexagon is considered 200 m to ensure that large maintenance ships can pass through. The system is designed spread along the coast, instead of perpendicular to the coast. This is to ensure as much as possible the same water depth across the system. In terms of dimensions, the length of the system is approximately 75 km and the width 13 km. A design of the overall system can be seen in figure 5.3:



Figure 5.3: Total System Layout

5.2.3. COST DRIVERS

In the previous sections, the final system configuration was selected. In this section, the cost of each component was analyzed in order to identify the main cost drivers of the project, which can be seen in figure 5.4.

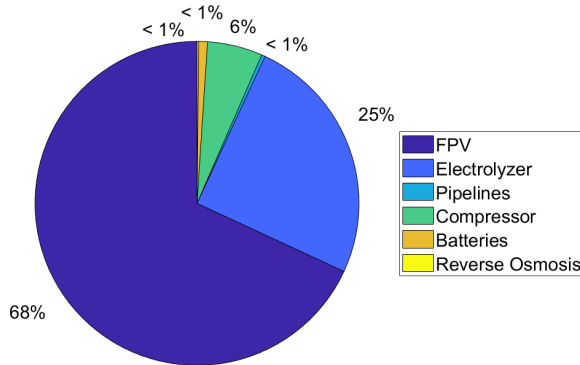


Figure 5.4: Contribution of system components to the LCOH

The main factor influencing the cost of the project is the FPV system, which accounts for 68 % of the project cost. The second main driving force of the project is the electrolyzer, which takes 25 % of the pie. Compressor contributes at a percentage of 6 %, while batteries, pipelines and reverse osmosis facilities account for less than 1% each. Therefore, the effect of the FPV system and the electrolyzer in the LCOH should be examined in more detail.

5.3. SENSITIVITY ANALYSIS

In this project, each component contributes on a different level to the LCOH calculation, as just presented. To simplify the calculations, several assumptions were made in this study, which could be a possible source of uncertainty. For this reason, a sensitivity analysis will be performed.

5.3.1. ASSUMPTIONS

Since the thesis, is an analysis of a project aiming for 2030, information about future cost and evolution of technologies are used, creating uncertainty. To make calculations simpler, assumptions were made, for the different values used in the system analysis. The main interest of the sensitivity is to analyse the main drivers contributing in the LCOH calculations. In section 5.2.3, the main cost factors were found to be the OFPV system

and the electrolyzer. Therefore, the assumptions used for the cost and size calculation of these two components will be discussed.

EFFICIENCY OF THE PV MODULES

PV module efficiency differs among the technologies. Crystalline-silicon PV modules are mostly used in energy projects. However, there are new technologies, such as perovskites, which are currently in the lab scale, promising higher efficiencies in the next years. In this research, the module efficiency considered is the best module efficiency in the lab at the moment (24.4 %), with the assumption that it will be the commercial value by 2030. However, improvements in PV technology are announced every day, with solar cell efficiencies reaching even 27 % already. Therefore, higher efficiency values are possible to be achieved by 2030. So, the effect of greater or smaller increase in the efficiency value must be examined. A +/- 20% change will be investigated.

COST OF THE PV SYSTEM

Land-based PV is a commercial technology, with hundreds of GWs installed worldwide. This is not the case for offshore floating PV projects. In addition, since this research is planned for 2030, a lot of values might be different. The cost of the OFPV system consists of the cost of the PV modules and the costs of the balance of system, including floating structures, mooring lines, anchors and power electronics as well as the installation costs. PV modules price are widely known and low risk projections were made for this value. To begin with, the cost of the PV panels was assumed to be 0.15 €/kW. However, this value is ambiguous, since price development cannot be projected precisely. Technology development and reductions on the price due to increased cumulative production, may lead in lower values. On the other hand, in case the development is not the expected, the cost values might be higher. The case is even more complicated for the balance of system cost, since OFPV projects are in a starting level in the market, and therefore, cost assumptions are hardly based on real data. Overall, a 30% increase/ decrease of the selected value will be investigated.

COST OF THE ELECTROLYZER

Electrolyzers' cost is significantly high and they are one of the main obstacles in designing hydrogen production systems. However, massive production might reduce the price of the electrolyzers. For this research, the electrolyzer cost is considered to be reduced to 200 €/kW. However, this price is an estimate based on literature data and learning curves of electrolyzers. Learning curves of other technologies, such as PV, show that this estimates might be too conservative, and therefore, it should be examined what would be the effect of a lower value. On the other hand, massive production might not drop the electrolyzer costs as expected, and therefore, a higher cost value should also be investigated. Overall, a 30% increase/ decrease of the selected value will be examined.

ELECTROLYZER FOOTPRINT

Electrolyzer footprint is an important parameter in hydrogen projects, especially offshore, where floating structures are needed. To determine how many floating structures are actually needed to provide buoyancy to the electrolyzer facility, the selection was based on assumptions based on specific data and sources. However, since such a large

scale system has not been designed and installed offshore, this uncertainty should be taken into account. Therefore it will be examined, how significantly will the cost be affected in the case that one floating barge will be used, or four floating barges will be used.

WACC

The weighted average cost of capital (WACC) used in this research is 3%. This is a typical value for renewable energy projects of mature renewable energy technologies. Since, this project is a future project, the future WACC cannot be projected. Huge development in PV and hydrogen technologies may drop this value even further. On the other hand, this projections might be too optimistic for some technologies of the proposed system, and the WACC value may not reach this level. Therefore, a sensitivity analysis needs to be performed, to examine all the scenarios. The effect of WACC rates of 2% and 5% is examined.

5.3.2. SENSITIVITY

In table 5.4, all the values used for the sensitivity analysis are presented. First, the selected value, and then, the optimistic case, in which the value is improved in the future and the pessimistic case, where this value will not have the expected development.

Table 5.4: Sensitivity parameters for pessimistic and optimistic values

Parameter	Selected Value	Optimistic	Pessimistic	
PV module efficiency	24.4	29.28 (+20 %)	19.52 (-20 %)	%
FPV System Cost	0.4	0.28 (-30 %)	0.52 (+30 %)	€/Wp
Electrolyzer Cost	200	140 (-30 %)	260 (+30 %)	€/kW
Barges Needed	2	1	4	
WACC	3	2	5	%

A cost sensitivity analysis is performed for the levelized cost of hydrogen (LCOH) by changing key input parameters and assumptions. The sensitivity parameters are based on an optimistic scenario and a pessimistic scenario. The main target is to identify the main cost drivers of the project and what would be the outcome if their values will be different in the future. In figure 5.5, the results of the sensitivity analysis are presented.

As can be noticed, the cost of the FPV system is the main driver of the project. A further decrease in the cost by 30%, leads in 19% decrease in the LCOH. PV efficiency follows the way, since a 20% future increase in the selected value, will lead in 10% reduced LCOH. WACC's contribution is also significant, since in case the rate for renewable energy projects is 5% instead of 3%, then the LCOH will be increased by 18%. Finally, the electrolyzer cost is not affecting the LCOH significantly, since a 30% decrease, leads to a 7% decreased LCOH, and the electrolyzer footprint, affecting the number of barges of

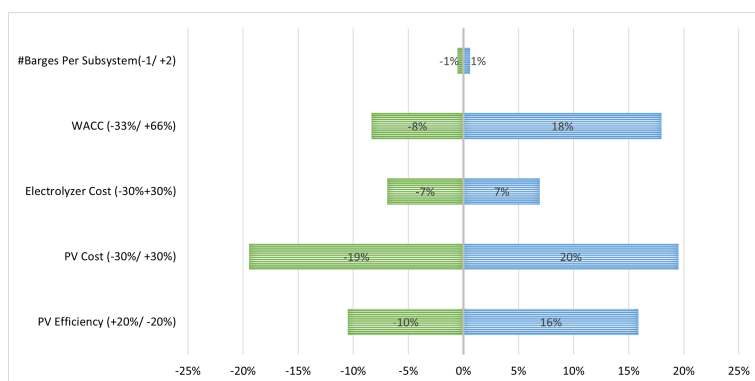


Figure 5.5: Sensitivity Analysis of the different values affecting the LCOH

the system, does not have a significant change in the cost of the system, resulting in a change of 1%.

5

Since FPV system cost is the main cost driver, further analysis must be performed to identify which part influences LCOH the most. The detailed effect of the cost of the FPV system main parts in the LCOH can be seen in figure 5.6:

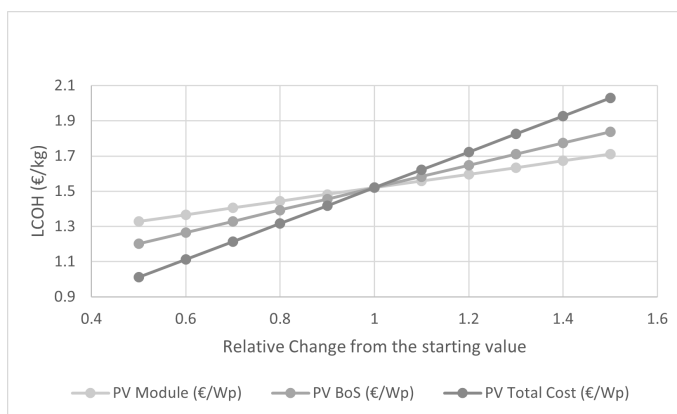


Figure 5.6: Sensitivity Analysis of the FPV system Cost

From the figure, it can be seen that the balance of system costs of the FPV system have greater influence on the LCOH than the PV module costs. This shows that the uncertainty around costs such as the floating structures, the mooring and anchoring system or the power electronics, affect significantly the cost of the project.

5.4. SCENARIO ANALYSIS

After investigating the sensitivity of the main scenario, which was based on realistic data and close to reality projections for 2030, two different scenarios will be also examined.

The optimistic scenario, which assumes important technology progress and cost reductions, and the pessimistic scenario, which assumes that technology and economies of scale will not have the progress assumed in the beginning. The scenarios will be based on realistic improvements in technology and prices of the main cost drivers of the project.

For the optimistic scenario, 20% decrease in FPV and electrolyzer costs is considered, along with 20 % increase in FPV system efficiency. Finally, the WACC is assumed to be decreased further to 2 %. For the pessimistic scenario, the worst possible values found in the literature, are used. The results can be seen in table 5.5:

Table 5.5: Scenario Data

Parameter	Base Scenario	Optimistic Scenario	Pessimistic Scenario	
PV efficiency	24.4	29.28	20	%
FPV Cost	0.4	0.32	0.5	€/Wp
El Cost	200	160	400	€/kW
WACC	3	2	5	%
LCOH	1.5	1.1	2.9	€/kg

6

DISCUSSION

Overall, an offshore hydrogen production system based on floating solar energy for the production of 1 million tons of hydrogen was proposed and studied. Background information was provided and the system was modelled in Matlab and Simulink software. Simulations were run for four different system configurations in order to identify the most cost-effective solution. By comparing the different configurations, it was found that a system based on alkaline electrolysis and without using batteries as an energy buffer, is capable of producing hydrogen at a competitive price. In this chapter, discussion about the results, the data, the assumptions used and other considerations will be addressed.

To begin with, it should be highlighted that all the assumptions are based on present knowledge and estimates about future developments. Therefore, values such as the PV module efficiency, the electrolyzer efficiency or the future costs of the technologies may vary significantly in the future. By performing a sensitivity analysis to the most contributing factors, this gap was filled.

In general, batteries provide better energy usage in the system. With the batteries involvement, the electrolyzers could operate at the rated capacity throughout all the year, even in low irradiance and night hours, something meaning that much less electrolyzer capacity is needed. More specifically, if the system operates 8760 hours per year, 5.42 GW of electrolysis are needed. Assuming a worst case scenario day of 16 consecutive hours of no sunlight, it is calculated that approximately 105 GWh of battery capacity is needed. This is an extreme amount of batteries since it represents almost 25 % of the current lithium-ion battery production (455 GWh) [107], which is not even used only for energy projects. In addition, in order to charge this amount of battery capacity, an excessive amount of PV should also be added. Therefore, the system cost will also be significantly higher, since batteries and PV are much more expensive than electrolyzers. After this quick analysis, it was decided that it may not be worth to examine the battery involvement in the system as an energy buffer and to focus on using batteries to store excess energy and power the electrolyzers during the night.

After comparing the different system configurations, the ones including batteries

were found to be the most expensive. Batteries operate as an energy buffer, storing the excess energy during the day and using it to power the electrolyzers during the night. Running the electrolyzers at constant load during all the hours of the year, would require an extravagant amount of batteries, and therefore this strategy was not tested. Batteries were used, in order to run the electrolyzer during the night at the minimum capacity. This way, electrolyzer operates almost throughout all the year, and less energy is wasted from the system. However, in terms of cost, batteries should be avoided, since their high cost increases the LCOH significantly.

Electrolyzers usually need some time in order to open/close and to change their operating levels. For alkaline electrolyzers, this can take some minutes, while for PEM some seconds are needed [32]. In this research, hourly data was used, and therefore, such delays were neglected. The same happens with the maintenance procedures of the electrolyzers. Electrolyzers typically need 5 days of maintenance per year [32]. However, since in this research, they shut down during the night, it is assumed that the maintenance will be planned then.

At this point, it is worth mentioning that through optimization processes, better sizing and control strategies could be identified. For instance, better ways of sizing the PV-electrolyzer system could be found, leading to even lower total costs. However, optimization was not part of this analysis and neither the target was to identify the precise solution to the problem.

Electrolyzers need pure water to operate as indicated several times through this report. For this reason a water treatment facility based on reverse osmosis is used. A water buffer tank is needed between the reverse osmosis installation and the electrolyzers, which was not included in the cost calculation. However, it is not expected that it would affect the costs significantly.

The final system size is calculated to be 32.6 GW for the PV system 22 GW for the electrolyzer. Comparing this data with maximum existing capacities, it is found that in practice, the largest PV system in the world is 2.2 GW [108], while OFPV projects are not even in a commercial level yet. Plus, hydrogen projects based on water electrolysis do not currently exceed MW scale. Looking at the largest green hydrogen projects announced, most of the projects are based on both wind and solar energy, and therefore, a safe comparison cannot be performed. However, for the HyDeal Ambition, 95 GW of PV are required to power 67 GW of electrolyzers for producing 3.6 million tonnes of H_2 per year [11]. Normalizing this values for 1 million tonnes per year, 24.4 GW of PV for 18.6 GW of electrolyzers are required. Therefore, in this study for 1 GW of electrolysis 1.48 GW of FPV are needed, while in the HyDeal project 1.3 GW of PV are needed. Therefore, the calculated size is comparable and similar, especially if the larger size and the different PV layout is considered.

It is also interesting to compare the PV capacity calculated with the projected capacity for 2030. More specifically it represents approximately 1% of the projected cumulative PV capacity for 2030, which according to IRENA is 2840 GW [109].

The economic results found in this research, show that it is possible to produce hydrogen in the selected location by 2030, for 1.5 €/kg. This price is in the same range with the grey hydrogen production costs, which is 1-2 €/kg, depending on the fossil fuels price [6]. Irena states that adding carbon capture technologies to fossil fuel based pro-

duction, increases the cost to 1.5-2.5 €/kg [9]. In the same report it is stated, that by 2030, average hydrogen cost from solar energy will be around 2.5-3 €/kg. Bloomberg New Energy Finance states that with an increase in production of electrolyzers, the hydrogen production costs could drop to 1.2 - 2.5 €/kg by 2030 [10] [110].

This price can be compared with several studies/projects announced. To begin with, HyDeal Ambition project aims for 1.50 €/kg for 2030 [11], a result close to the one calculated in this research. An interesting comparison could be with hydrogen produced by wind and solar systems in North Africa, where electricity costs are much lower than Europe, at sites with good solar and wind resources. The hydrogen production costs in North Africa are expected to be around 1 €/kg by 2030 [111]. In Europe, however, where energy production costs are higher, the hydrogen production costs are expected to be around 1.5-2 €/kg [111]. The LCOH calculated in this research is in the range projected for the European zone, and higher than the one projected for Africa, which is reasonable based on the more favourable solar irradiation condition in Africa than Europe.

7

CONCLUSION & RECOMMENDATIONS

7.1. CONCLUSION

The goal of this research was to evaluate the techno-economic feasibility of a Power to Gas system based on floating solar energy for green hydrogen production, located in Greece. At first, a literature study was performed in order to examine the current green hydrogen projects and identify background information on hydrogen production systems and FPV technologies. From the information collected about the different components of the system, sizing and cost details were determined for each one of the components. Afterwards, a model was designed in Matlab and Simulink software including sizing of all the components and calculation of the LCOH. To summarize, the sub-questions addressed in the introduction of the report, will be answered, leading the way to answering the main research question:

1. **What are the main system components of an offshore solar to hydrogen system?**

The hydrogen production is based on water electrolysis. The power is supplied from an offshore floating photovoltaic system. Due to the intermittent power output of the PV system and given the fact that water electrolyzers are preferred to run on a steady power supply, batteries can be used. The electrolyzer unit requires pure water to operate and therefore, a water treatment unit based on reverse osmosis is needed. The produced hydrogen will be injected into the hydrogen network. To do so, the hydrogen should be pressurized to 100 bars. Therefore, a compressor facility to increase the pressure from the electrolyzer output to 100 bars is needed. Finally, pipelines are used in order to transfer the compressed hydrogen to the main pipeline grid.

2. **What are the main challenges for the technical and financial feasibility of the proposed hydrogen system?**

To answer this question, a literature study was performed. In the literature, there are no such existing projects yet. This is mostly due to the niche level of the OFPV technology and the high capital costs of electrolyzers at the moment. Therefore, a lot of information were based on assumptions for the technological and cost developments projected for the future, something that creates a lot of uncertainty around the project. The main challenges that came out from the literature are both technical and cost related. From the technical side, offshore environment proposes several environmental challenges such as strong winds and deep waters. Therefore, floating structures able to withstand extreme environmental conditions should be selected. Currently, there are no commercial projects including OFPV. Therefore, the system was mostly designed based on information and assumptions of inland floating and land-based PV systems. Regarding the electrolyzers, the fact that they operate with constant load input, makes a temporary energy storage addition such as batteries, a reasonable consideration. From a technology perspective, alkaline and PEM are the two commercially available electrolyzer technologies. Alkaline have better efficiency and lower cost, while PEM have more compact design, which is more useful in offshore projects. In terms of cost, since the project is designed for 2030, there many uncertainties. PV module's cost is declining continuously and is expected to decline even more as the production is increasing. However, the landscape on the balance of system costs for the FPV system is not clear, since there are no relevant projects in the literature. On the electrolyzer part, currently projects do not exceed MW scale, and therefore, information on economies of scale effect on the electrolyzer prices are not available.

3. What is the proper way to model the proposed hydrogen system?

This question was answered in section 4. A model was created using Matlab and Simulink software. The model starts with the power calculation of the FPV system. Then, it decides how the power is distributed through the system, based on the control strategy designed and implemented. Then the hydrogen production for one year is calculated. Finally, the total costs (€/yr) are calculated based on the capex, the operation and maintenance costs of each components and the WACC. From this values, the LCOH (€/kg) of the proposed system is calculated.

4. What is the most cost-effective system configuration?

After modeling the different system configurations and running the simulations on Matlab and Simulink, the results presented on table 7.1 are calculated. From this, it can be concluded that the most cost-effective configuration is the one based on alkaline electrolyzer technology without the use of batteries as an energy buffer.

Table 7.1: LCOH of the four different configurations

	Alkaline & No Battery	Alkaline & Battery	PEM & No Battery	PEM & Battery
LCOH (€/kg)	1.5	2.0	1.8	2.2

An overview of the final system can be seen in figure 7.1:

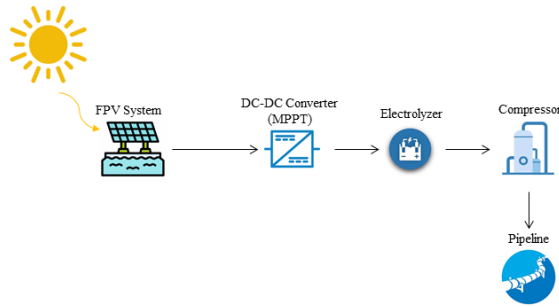


Figure 7.1: Overview of the final system configuration

5. What is the economic feasibility of the proposed system to produce one million ton of hydrogen in an area north to Crete?

The results for the final system configuration proved that it is feasible to produce 1 million tons of hydrogen per year based on offshore floating solar energy, north to Crete island in Greece, with a cost of 1.5 €/kg, in 2030. This result is comparable to announced projects for the same year and also to blue hydrogen production costs.

6. What are the main cost drivers to reduce the overall LCOH of the system?

The main cost drivers of the project are the OFPV system, contributing at 68% of the total LCOH, and the electrolyzer, accounting for 25% of the LCOH. Going through one more level of detail, the main factors influencing the cost of the system are the cost of the FPV system, the PV module efficiency and the electrolyzer cost. More specifically, if the FPV system cost is reduced by 30% from the considered value, the LCOH can drop by 19%. If the PV module efficiency increases by 20% from the considered value, the LCOH can drop by 10%. Finally, If the electrolyzer cost drops by 30%, the LCOH can be reduced by 7%.

Finally, the main research question was answered:

What is the cost of producing 1 million tons of hydrogen per year from floating solar energy, in an area north of Crete?

This study concludes that a hydrogen production system based on offshore floating solar energy, located north to Crete, in the Aegean Sea, can produce green hydrogen at the competitive price of 1.5 €/kg. The most cost-efficient system layout includes alkaline electrolyzers and does not use batteries as an energy buffer. For the FPV system, the membrane proposed by the Ocean Sun was selected as a floating structure, due to the technology readiness level, compared to other technologies. The rest of the system includes reverse osmosis facilities for highly pure water, compressors for increasing the pressure of the produced hydrogen and pipelines for the hydrogen injection into the European pipeline network. It should be mentioned that a small amount of batteries is used to keep the control systems open during the low irradiance and night hours. Finally, floating barges are used to provide buoyancy to the electrolyzers, the compressors, the reverse osmosis facilities and the batteries. Regarding the cost analysis, OFPV system

price has the largest influence on the LCOH. Overall, from this research it is clear that the proposed hydrogen production system can produce cost-competitive green hydrogen.

7.2. FUTURE RESEARCH RECOMMENDATIONS

The following recommendations for future research are proposed. To begin with, this study was one of the few available in the green hydrogen production field based on floating solar energy, and the first full research based on offshore floating solar for offshore hydrogen production. Therefore, one can easily understand that for many parts of this research, a more general level of detail was used, since the target was to give a first impression of how much such a system costs, and not examine it in detail. Some possible recommendations for future research are:

- Using a different model for the FPV system power output calculation. In this study, the simple efficiency model was used, taking into account the temperature effect on the efficiency. However, there are other models existing, which provide higher level of detail on the power output calculation.
- Examining the electrolyzer efficiency, which was considered constant, in more detail. In practice, the electrolyzer efficiency varies depending on the input load. Therefore, for future research, it might be worth investigating in more detail, what would be the effect of the electrolyzer variable efficiency based on partial load operation in the hydrogen production process.
- Optimization of the system sizing. As commented in various sections across this thesis, the sizing was done manually, based on the LCOH results. However, there might be a more optimal way of component sizing, that could possibly result in decreased costs. Therefore, by using optimization techniques, even reduced costs might be found.

BIBLIOGRAPHY

- [1] *Key aspects of the paris agreement*, Online; accessed 5 June 2021. [Online]. Available: <https://unfccc.int/process-and-meetings/the-paris-agreement/the-paris-agreement/key-aspects-of-the-paris-agreement>.
- [2] A. Abdalla, S. Hossain, O. Nisfindy, A. Azad, M. Dawood, and A. Azad, "Hydrogen production, storage, transportation and key challenges with applications: A review," *Energy Conversion and Management*, vol. 165, pp. 602–627, Jun. 2018.
- [3] Y. Zhang, Z. Jia, Z. Yuan, T. Yang, Y. Qi, and D. Zhao, "Development and application of hydrogen storage," *Journal of Iron and Steel Research, International*, vol. 22, no. 9, pp. 757–770, 2015.
- [4] R. Boudries, A. Khellaf, A. Aliane, L. Ihaddaden, and F. Khida, "Pv system design for powering an industrial unit for hydrogen production," *International Journal of Hydrogen Energy*, vol. 39, no. 27, pp. 15 188–15 195, 2014.
- [5] P. Nikolaidis and A. Poullikkas, "A comparative overview of hydrogen production processes," *Renewable and Sustainable Energy Reviews*, vol. 67, pp. 597–611, 2017.
- [6] IEA, *The future of hydrogen (2019 report)*, <https://www.iea.org/reports/the-future-of-hydrogen>, Online; accessed 15 February 2021.
- [7] S. E. Hosseini and M. A. Wahid, "Hydrogen production from renewable and sustainable energy resources: Promising green energy carrier for clean development," *Renewable and Sustainable Energy Reviews*, vol. 57, pp. 850–866, 2016.
- [8] Irena, *Renewable energy sources*, <https://www.irena.org/>, Online; accessed 3 December 2020.
- [9] —, "Hydrogen: A renewable energy perspective," 2019.
- [10] "Hydrogen: The economics of production from renewables," *Bloomberg New Energy Finance*, 2019.
- [11] *Global green-hydrogen pipeline exceeds 200gw — here's the 24 largest gigawatt-scale projects*, Online; accessed 5 July 2021. [Online]. Available: <https://www.rechargenews.com/energy-transition/global-green-hydrogen-%5C%5Cpipeline-exceeds-200gw-heres-the-24-largest-gigawatt-scale-projects/2-1-933755>.
- [12] E. Kabir, P. Kumar, S. Kumar, A. A. Adelodun, and K.-H. Kim, "Solar energy: Potential and future prospects," *Renewable and Sustainable Energy Reviews*, vol. 82, pp. 894–900, 2018, ISSN: 1364-0321.
- [13] EMODnet, *Bathymetry*. [Online]. Available: <https://www.emodnet-bathymetry.eu/>.

- [14] G. Lavidas and V. Venugopal, "A 35 year high-resolution wave atlas for nearshore energy production and economics at the aegean sea," *Renewable Energy*, vol. 103, pp. 401–417, 2017.
- [15] A. Zacharioudaki, G. Korres, and L. Perivoliotis, "Wave climate of the hellenic seas obtained from a wave hindcast for the period 1960 - 2001," *Ocean Dynamics*, vol. 65, pp. 795–816, 2015.
- [16] "Photovoltaic geographical information system," Online; accessed 25 May 2021.
- [17] G. S. Atlas. [Online]. Available: <https://globalsolaratlas.info/map>.
- [18] G. Tjarks, J. Mergel, and D. Stolten, "Dynamic operation of electrolyzers: Systems design and operating strategies," in *Hydrogen Science and Engineering : Materials, Processes, Systems and Technology*. John Wiley Sons, Ltd, 2016, ch. 14, pp. 309–330, ISBN: 9783527674268. DOI: <https://doi.org/10.1002/9783527674268.ch14>. eprint: <https://onlinelibrary.wiley.com/doi/pdf/10.1002/9783527674268.ch14>. [Online]. Available: <https://onlinelibrary.wiley.com/doi/abs/10.1002/9783527674268.ch14>.
- [19] A. Buttler and H. Spliethoff, "Current status of water electrolysis for energy storage, grid balancing and sector coupling via power-to-gas and power-to-liquids: A review," *Renewable and Sustainable Energy Reviews*, vol. 82, pp. 2440–2454, 2018, ISSN: 1364-0321. DOI: <https://doi.org/10.1016/j.rser.2017.09.003>. [Online]. Available: <https://www.sciencedirect.com/science/article/pii/S136403211731242X>.
- [20] M. Becker, J. Brauns, and T. Turek, "Battery-buffered alkaline water electrolysis powered by photovoltaics," *Chemie Ingenieur Technik*, vol. 93, no. 4, pp. 655–663, 2021. DOI: <https://doi.org/10.1002/cite.202000151>. eprint: <https://onlinelibrary.wiley.com/doi/pdf/10.1002/cite.202000151>. [Online]. Available: <https://onlinelibrary.wiley.com/doi/abs/10.1002/cite.202000151>.
- [21] "Hydrogen insights: A perspective on hydrogen investment, market development and cost competitiveness," *Journal of Physics: Conference Series*, Feb. 2021.
- [22] P. S. A. Ursua L. M. Gandia, "Hydrogen production from water electrolysis: Current status and future trends," *Proceedings of the IEEE*, vol. 100, pp. 410–426, 2012.
- [23] J. Chi and H. Yu, "Water electrolysis based on renewable energy for hydrogen production," *Chinese Journal of Catalysis*, vol. 39, no. 3, pp. 390–394, 2018.
- [24] *Hydrogen production: Electrolysis*, <https://www.energy.gov/>, Online; accessed 15 February 2021.
- [25] H. J. V.-H. N. A. Lopez-Garcia M. E. Rodríguez-Tapia and G. M. Chávez-Campos, "Water electrolysis experimental characterization and numerical model: Case of study with three kind of electrodes," *IEEE International Autumn Meeting on Power, Electronics and Computing (ROPEC)*, pp. 1–4, 2017.
- [26] E. Zoulias, E. Varkaraki, N. Lymberopoulos, C. Christodoulou, and G. Karagiorgis, "A review on water electrolysis," *TCJST*, vol. 4, pp. 41–71, Jan. 2004.

- [27] I. Dincer, "Green methods for hydrogen production," *International Journal of Hydrogen Energy*, vol. 37, no. 2, pp. 1954–1971, 2012.
- [28] "Integration of gigawatt scale electrolyser in five industrial clusters," *Institute for Sustainable Process Technology (ISPT)*, 2020.
- [29] IEA, "The future of hydrogen: Seizing today's opportunities," 2019.
- [30] "Strategic research and innovation agenda: Final draft," *Hydrogen Europe*, 2020.
- [31] Hydrogenics, "Hydrogenics: Hystat® technical specifications," Online; accessed 10 May 2021.
- [32] "Study on development of water electrolysis in the EU," *E4tech with Element Energy Ltd*, 2014.
- [33] E4Tech, "Development of water electrolysis in the european union," *Fuel Cells and Hydrogen Joint Undertaking*, 2014.
- [34] DNV, "Power-to-hydrogen ijmuiden ver: Final report for tennet and gasunie," 2018.
- [35] K. Donkers, "Hydrogen production on offshore platforms: A techno-economic analysis," *Utrecht University*, 2020.
- [36] Irena, "Green hydrogen cost reduction: Scaling up electrolysers to meet the 1.5°C climate goal," 2020.
- [37] O. Schmidt, A. Gambhir, I. Staffell, A. Hawkes, J. Nelson, and S. Few, "Future cost and performance of water electrolysis: An expert elicitation study," *International Journal of Hydrogen Energy*, vol. 42, no. 52, pp. 30 470–30 492, 2017.
- [38] "An overview of hydrogen production technologies," *Catalysis Today*, vol. 139, no. 4, pp. 244–260, 2009.
- [39] Shell, *Shell hydrogen study: Energy of the future*, 2017.
- [40] M. K., "Hydrogen production with sea water electrolysis using norwegian offshore wind energy potentials," *Int J Energy Environ Eng*, vol. 5, pp. 104–116, 2014.
- [41] Ivaro Serna and F. Tadeo, "Offshore hydrogen production from wave energy," *International Journal of Hydrogen Energy*, vol. 39, no. 3, pp. 1549–1557, 2014, ISSN: 0360-3199.
- [42] R. Roobeek, "Shipping sunshine," 2020. [Online]. Available: <http://resolver.tudelft.nl/uuid:9d1225b7-65ed-44d2-b9c9-d60cfce64a5f>.
- [43] J. Hogerwaard, I. Dincer, G. F. Naterer, and B. D. Patterson, "Solar methanol synthesis by clean hydrogen production from seawater on offshore artificial islands," *International Journal of Energy Research*, vol. 43, no. 11, pp. 5687–5700, 2019. DOI: <https://doi.org/10.1002/er.4627>. eprint: <https://onlinelibrary.wiley.com/doi/pdf/10.1002/er.4627>. [Online]. Available: <https://onlinelibrary.wiley.com/doi/abs/10.1002/er.4627>.

- [44] U. Caldera and C. Breyer, "Learning curve for seawater reverse osmosis desalination plants: Capital cost trend of the past, present, and future," *Water Resources Research*, vol. 53, no. 12, pp. 10 523–10 538, 2017. DOI: <https://doi.org/10.1002/2017WR021402>. eprint: <https://agupubs.onlinelibrary.wiley.com/doi/pdf/10.1002/2017WR021402>. [Online]. Available: <https://agupubs.onlinelibrary.wiley.com/doi/abs/10.1002/2017WR021402>.
- [45] R. Moradi and K. M. Groth, "Hydrogen storage and delivery: Review of the state of the art technologies and risk and reliability analysis," *International Journal of Hydrogen Energy*, vol. 44, no. 23, pp. 12 254–12 269, 2019.
- [46] *Natural gas supply association*, <https://www.naturalgas.org>, Online; accessed 15 June 2021.
- [47] Irena, "Renewable power generation costs in 2019," 2020.
- [48] A. Smets, K. Jäger, O. Isabella, R. van Swaaij, and M. Zeman, *Solar Energy: The Physics and Engineering of Photovoltaic Conversion, Technologies and Systems*. UIT Cambridge, 2016.
- [49] *Solar cell operation*, <https://www.pveducation.org/>, Online; accessed 21 February 2021.
- [50] A. Sahu, N. Yadav, and K. Sudhakar, "Floating photovoltaic power plant: A review," *Renewable and Sustainable Energy Reviews*, vol. 66, pp. 815–824, 2016.
- [51] WorldBankGroup and SERIS, *Where Sun Meets Water, Floating Solar Market Report*. 2018.
- [52] AkuoEnergy, *Hydrelia floating solar panel*, <https://www.akuoenergy.com/en>, Online; accessed 15 January 2021.
- [53] O. of Energy, *Offshore floating solar farm installed and operational at the dutch north sea*, <https://oceansofenergy.blue/>, Online; accessed 15 January 2021.
- [54] N. Lee, U. Grunwald, E. Rosenlieb, H. Mirletz, A. Aznar, R. Spencer, and S. Cox, "Hybrid floating solar photovoltaics-hydropower systems: Benefits and global assessment of technical potential," *Renewable Energy*, vol. 162, pp. 1415–1427, 2020.
- [55] S. Pinto and J. Stokkermans, "Marine floating solar plants: An overview of potential, challenges and feasibility," *Proceedings of the Institution of Civil Engineers - Maritime Engineering*, vol. 173, pp. 1–39, Jul. 2020.
- [56] T. L. Gibson and N. A. Kelly, "Optimization of solar powered hydrogen production using photovoltaic electrolysis devices," *International Journal of Hydrogen Energy*, vol. 33, no. 21, pp. 5931–5940, 2008, ISSN: 0360-3199. DOI: <https://doi.org/10.1016/j.ijhydene.2008.05.106>. [Online]. Available: <https://www.sciencedirect.com/science/article/pii/S0360319908006526>.
- [57] "Novel offshore application of photovoltaics in comparison to conventional marine renewable energy technologies," *Renewable Energy*, vol. 50, pp. 879–888, 2013.
- [58] "Photovoltaics report," *Fraunhofer Institute for Solar Energy Systems, ISE with support of PSE Projects GmbH*, 2021.

- [59] “Photovoltaics report,” *Fraunhofer Institute for Solar Energy Systems, ISE with support of PSE Projects GmbH*, 2020.
- [60] E. Vartiainen, G. Masson, C. Breyer, D. Moser, and E. Romn Medina, “Impact of weighted average cost of capital, capital expenditure, and other parameters on future utility-scale pv levelised cost of electricity,” *Progress in Photovoltaics: Research and Applications*, vol. 28, no. 6, pp. 439–453, 2020. DOI: <https://doi.org/10.1002/pip.3189>. eprint: <https://onlinelibrary.wiley.com/doi/pdf/10.1002/pip.3189>. [Online]. Available: <https://onlinelibrary.wiley.com/doi/abs/10.1002/pip.3189>.
- [61] PVinsights, <http://pvinsights.com/>, Online; accessed 10 May 2021.
- [62] L. Oberbeck, K. Alvino, B. Goraya, and M. Jubault, “Ipv’s pv technology vision for 2030,” *Progress in Photovoltaics: Research and Applications*, vol. 28, no. 11, pp. 1207–1214, 2020. DOI: <https://doi.org/10.1002/pip.3305>. eprint: <https://onlinelibrary.wiley.com/doi/pdf/10.1002/pip.3305>. [Online]. Available: <https://onlinelibrary.wiley.com/doi/abs/10.1002/pip.3305>.
- [63] S. Oliveira-Pinto and J. Stokkermans, “Assessment of the potential of different floating solar technologies – overview and analysis of different case studies,” *Energy Conversion and Management*, vol. 211, p. 112 747, 2020.
- [64] OceanSun, *Projects*, <https://oceansun.no/>, Online; accessed 15 February 2021.
- [65] N. Ravichandran, N. Ravichandran, and B. Panneerselvam, “Floating photovoltaic thin film technology—a review,” pp. 329–338, Feb. 2020.
- [66] K. Trapani and D. Millar, “Hydrodynamic overview of flexible floating thin film pv arrays,” Jul. 2016.
- [67] R. Cazzaniga, M. Cicu, M. Rosa-Clot, P. Rosa-Clot, G. Tina, and C. Ventura, “Floating photovoltaic plants: Performance analysis and design solutions,” *Renewable and Sustainable Energy Reviews*, vol. 81, pp. 1730–1741, 2018.
- [68] X. Wu, Y. Hu, Y. Li, J. Yang, L. Duan, T. Wang, T. Adcock, Z. Jiang, Z. Gao, Z. Lin, A. Borthwick, and S. Liao, “Foundations of offshore wind turbines: A review,” *Renewable and Sustainable Energy Reviews*, vol. 104, pp. 379–393, 2019, ISSN: 1364-0321. DOI: <https://doi.org/10.1016/j.rser.2019.01.012>. [Online]. Available: <https://www.sciencedirect.com/science/article/pii/S1364032119300127>.
- [69] T. Whittaker, M. Folley, and J. Hancock, “Chapter 5 - environmental loads, motions, and mooring systems,” in *Floating PV Plants*, M. Rosa-Clot and G. Marco Tina, Eds., Academic Press, 2020, pp. 47–66, ISBN: 978-0-12-817061-8. DOI: <https://doi.org/10.1016/B978-0-12-817061-8.00005-1>. [Online]. Available: <https://www.sciencedirect.com/science/article/pii/B978012817065C%5C18000051>.

- [70] Irena, *Utility-scale batteries: Innovation landscape brief*, <https://www.irena.org/publications/2019/Sep/Utility-scale-batteries>, Online; accessed 28 April 2021.
- [71] *Battery cell comparison*, Online; accessed 5 July 2021. [Online]. Available: <https://www.epectec.com/batteries/cell-comparison.html>.
- [72] BNEF, *Battery pack prices cited below \$100/kwh for the first time in 2020, while market average sits at \$137/kwh*, <https://about.bnef.com/blog/battery-pack-prices-cited-below-100-kwh-for-the-first-time-in-2020-while-market-average-sits-at-137-kwh/>, Online; accessed 28 April 2021.
- [73] Irena, *Battery storage technology improvements and cost reductions to 2030: A deep dive*, Online; accessed 28 April 2021.
- [74] *Electricity storage and renewables: Costs and markets to 2030*, https://www.irena.org/-/media/Files/IRENA/Agency/Publication/2017/Oct/IRENA_Electricity_Storage_Costs_2017.pdf, 2017.
- [75] J. van der Blonk, *Feasibility of a floating green battery: Concept design for the green battery on the energy storage lake of the delta21 project*, 2020. [Online]. Available: <http://resolver.tudelft.nl/uuid:bd356db8-0b0f-4756-93c6-caca7033c3a3>.
- [76] G. Perkins, "Techno-economic comparison of the levelised cost of electricity generation from solar pv and battery storage with solar pv and combustion of bio-crude using fast pyrolysis of biomass," *Energy Conversion and Management*, vol. 171, pp. 1573–1588, 2018, ISSN: 0196-8904. DOI: <https://doi.org/10.1016/j.enconman.2018.06.090>. [Online]. Available: <https://www.sciencedirect.com/science/article/pii/S0196890418307003>.
- [77] M. Leimeister, A. Kolios, and M. Collu, "Critical review of floating support structures for offshore wind farm deployment," *Journal of Physics: Conference Series*, vol. 1104, p. 012007, Oct. 2018. DOI: [10.1088/1742-6596/1104/1/012007](https://doi.org/10.1088/1742-6596/1104/1/012007). [Online]. Available: <https://doi.org/10.1088/1742-6596/1104/1/012007>.
- [78] *Damen shipyards group*, Online; accessed 5 June 2021. [Online]. Available: <https://www.damen.com/>.
- [79] B. Jha, *Different types of barges – uses and differences*, Online; accessed 5 June 2021. [Online]. Available: <https://www.marineinsight.com/types-of-ships/different-types-of-barges-used-in-the-shipping-world/>.
- [80] E. van Druten and K. Kruit, "Perspectieven elektriciteit uit water: Nationaal potentieel voor 2030 en 2050," 2019.
- [81] D. Feldman, V. Ramasamy, R. Fu, A. Ramdas, J. Desai, and R. Margolis, "U.S. solar photovoltaic system and energy storage cost benchmark: Q1 2020," Feb. 2021. DOI: [10.2172/1765601](https://doi.org/10.2172/1765601). [Online]. Available: <https://www.osti.gov/biblio/1765601>.
- [82] D. Feldman, V. Ramasamy, and R. Margolis, "U.S. solar photovoltaic bess system cost benchmark q1 2020 report," Jan. 2021. DOI: [10.7799/1762492](https://doi.org/10.7799/1762492). [Online]. Available: <https://www.osti.gov/biblio/1762492>.

- [83] T. R. Ran Fu and R. Margolis, “2018 U.S. utility-scale photovoltaicsplus-energy storage system costs benchmark,” *National Renewable Energy Laboratory*, 2018.
- [84] K. Trapani and D. L. Millar, “Proposing offshore photovoltaic (PV) technology to the energy mix of the Maltese islands,” *Energy Conversion and Management*, vol. 67, pp. 18–26, 2013, ISSN: 0196-8904. DOI: <https://doi.org/10.1016/j.enconman.2012.10.022>. [Online]. Available: <https://www.sciencedirect.com/science/article/pii/S0196890412004219>.
- [85] B. Bjørneklett, personal communication, May 3, 2021.
- [86] J. Armijo and C. Philibert, “Flexible production of green hydrogen and ammonia from variable solar and wind energy: Case study of Chile and Argentina,” *International Journal of Hydrogen Energy*, vol. 45, no. 3, pp. 1541–1558, 2020, ISSN: 0360-3199. DOI: <https://doi.org/10.1016/j.ijhydene.2019.11.028>. [Online]. Available: <https://www.sciencedirect.com/science/article/pii/S0360319919342089>.
- [87] D. C. R. Andreas Zauner Hans Böhm and R. Tichler, “Innovative large-scale energy storage technologies and power-to-gas concepts after optimization: Analysis on future technology options and on techno-economic optimization,” *Store&Go*, 2019.
- [88] Irena, *Hydrogen from renewable power: Technology outlook for the energy transition*, 2018.
- [89] M. A. Khan, I. Al-Shankiti, A. Ziani, and H. Idriss, “Demonstration of green hydrogen production using solar energy at 28% efficiency and evaluation of its economic viability,” *Sustainable Energy Fuels*, vol. 5, pp. 1085–1094, 4 2021. DOI: [10.1039/D0SE01761B](https://doi.org/10.1039/D0SE01761B). [Online]. Available: <http://dx.doi.org/10.1039/D0SE01761B>.
- [90] none, “Current (2009) state-of-the-art hydrogen production cost estimate using water electrolysis,” Sep. 2009. DOI: [10.2172/1218930](https://doi.org/10.2172/1218930). [Online]. Available: <https://www.osti.gov/biblio/1218930>.
- [91] L. Graré, “Hydrogen: Electrolysis empowering green hydrogen,” *NEL*, 2019.
- [92] I. Dickschas and T. Smolinka, “Wasserelektrolyse an der Schwelle zur großskaligen Industrialisierung – trends und Herausforderungen bis 2030,” *Fraunhofer Institute for Solar Energy Systems*, 2019.
- [93] SolarReviews, *What are the different types of solar batteries?* <https://www.solarreviews.com/blog/types-of-solar-batteries>, Online; accessed 10 January 2021.
- [94] “Towards sustainable energy production on the North Sea - green hydrogen production and CO₂ storage: Onshore or offshore?” *North Sea Energy*, 2018.

- [95] M. Wang, J. Peng, Y. Luo, Z. Shen, and H. Yang, "Comparison of different simplistic prediction models for forecasting pv power output: Assessment with experimental measurements," *Energy*, vol. 224, p. 120 162, 2021, ISSN: 0360-5442. DOI: <https://doi.org/10.1016/j.energy.2021.120162>. [Online]. Available: <https://www.sciencedirect.com/science/article/pii/S036054422100%5C%5C4114>.
- [96] W. Charles Lawrence Kamuyu, J. R. Lim, C. S. Won, and H. K. Ahn, "Prediction model of photovoltaic module temperature for power performance of floating pvs," *Energies*, vol. 11, no. 2, 2018, ISSN: 1996-1073. DOI: [10.3390/en11020447](https://doi.org/10.3390/en11020447). [Online]. Available: <https://www.mdpi.com/1996-1073/11/2/447>.
- [97] E. A. U. Anyanime Tim Umoette and M. U. Festus, "Design of stand alone floating pv system for ibeno health centre," *Science Journal of Energy Engineering*, vol. 4, no. 6, pp. 56–61, 2016. DOI: [10.11648/j.sjee.20160406.12](https://doi.org/10.11648/j.sjee.20160406.12).
- [98] S. Darling, F. You, T. Veselka, and A. Velosa, "Assumptions and the levelized cost of energy for photovoltaics," *Energy Environ. Sci.*, vol. 4, pp. 3133–3139, Aug. 2011. DOI: [10.1039/C0EE00698J](https://doi.org/10.1039/C0EE00698J).
- [99] B. Marion, J. Adelstein, K. Boyle, H. Hayden, B. Hammond, T. Fletcher, B. Canada, D. Narang, A. Kimber, L. Mitchell, G. Rich, and T. Townsend, "Performance parameters for grid-connected pv systems," in *Conference Record of the Thirty-first IEEE Photovoltaic Specialists Conference, 2005.*, 2005, pp. 1601–1606. DOI: [10.1109/PVSC.2005.1488451](https://doi.org/10.1109/PVSC.2005.1488451).
- [100] S. Touili, A. Alami Merrouni, A. Azouzoute, Y. El Hassouani, and A.-i. Amrani, "A technical and economical assessment of hydrogen production potential from solar energy in Morocco," *International Journal of Hydrogen Energy*, vol. 43, no. 51, pp. 22 777–22 796, 2018, ISSN: 0360-3199. DOI: <https://doi.org/10.1016/j.ijhydene.2018.10.136>. [Online]. Available: <https://www.sciencedirect.com/science/article/pii/S0360319918333639>.
- [101] T. Schoehuijs, "Direct coupling feasibility evaluation," *TU Delft*, 2018. [Online]. Available: <https://repository.tudelft.nl/islandora/object/uuid%5C%3Acb721f6f-236b-4039-93cd-a6762d8e146b>.
- [102] J. B. Néstor González Díez Simone van der Meer and A. Herwijn, "Technical assessment of hydrogen transport, compression, processing offshore," *North Sea Energy*, 2020.
- [103] D. Fernandes, "Exploring p2h futures in the north sea using spatially explicit, techno-economic modelling," 2020. [Online]. Available: <http://resolver.tudelft.nl/uuid:5c20b6d5-0a4b-4ce3-8880-5fb92434b954>.
- [104] *Engineering toolbox*, <https://www.engineeringtoolbox.com/>, Online; accessed 10 June 2021.
- [105] A. van Wijk, "Hydrogen, the bridge between Africa and Europe.," 2019.

- [106] K. K. Jens Mischner Hans-Georg Fasold, "Gas2energy.net: Systemplanerische Grundlagen der Gasversorgung inkl," *Deutscher Industrieverlag*, 2015. [Online]. Available: <https://www.sciencedirect.com/science/article/pii/S036031991%5C%5C93338625>.
- [107] A. Yu and M. Sumangil, *Top electric vehicle markets dominate lithium-ion battery capacity growth*, Online; accessed 5 September 2021. [Online]. Available: <https://www.spglobal.com/marketintelligence/en/news-insights/blog/top-electric-vehicle-markets-dominate-lithium-ion-battery-capacity-growth>.
- [108] *World's largest solar plant goes online in china — 2.2 gw*, Online; accessed 5 July 2021. [Online]. Available: <https://pv-magazine-usa.com/2020/10/02/worlds-largest-solar-plant-goes-online-in-china/>.
- [109] Irena, "Future of solar photovoltaic: Deployment, investment, technology, grid integration and socio-economic aspects," 2019.
- [110] A. Christensen, "Assessment of hydrogen production costs from electrolysis: United states and europe," *International Council of Clean Transportation*, 2020.
- [111] "A North Africa - Europe hydrogen manifesto," *Dii Desert Energy*, 2019.

A

APPENDIX

In this chapter, the model presented in chapter 4 will be verified. In general the model does not include complicated equations. Most of the equations are simple and therefore, the possibility of error is small. Before running the simulation of the model presented in chapter 4, with the final inputs, verification and validation of the model needs to be performed. In this chapter, it will be shown that the model designed in Matlab/Simulink software represents the equations introduced and analysed.

Normally, a model validation process should be performed as well. Model validation shows if the model can support what it stands for. Therefore, validation is about checking if equations, assumptions, figures and main theories are correctly used. However, the limited access to historical data relevant to this project, make the model validation difficult, if not impossible. In general, since the project studied in this research is a 2030 case and no similar studies or projects has been already performed, there are no available data to validate the model.

Therefore, only model verification will be shown, which consists of proving that the model outcome is the one supposed to be when designed. In simpler words, the target is to show that the model results/ figures are the same with the numbers calculated manually on the paper. The model that calculates the FPV system power output, the hydrogen production and the energy consumption of the compressor and the reverse osmosis facilities will be verified.

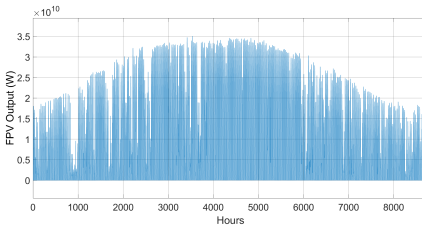
To begin with the verification process and starting from the FPV system power output check, comparison is performed between the power output of the floating PV model result and calculations made on paper. More specifically, by setting 3 different random hours through the year, hour 687, hour 3967 and hour 6750, tests were made to verify that the model calculated the results as it should. All the results can be seen in table A.1. As can be seen, the model calculates the results correctly, without any errors.

Apart from the number comparison, a graph behavior comparison was performed as well. The FPV power output (figure A.1), should have exactly the same form as the irradiance plot, presented in figure 1.6. By changing only the irradiance levels, it can be seen how the FPV system output varies. At first, it can be noticed, that for zero irradiance

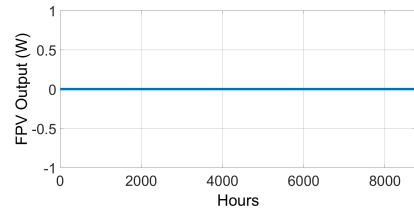
Table A.1: Model Verification

Value	Model 1	Paper 1	Model 2	Paper 2	Model 3	Paper 3	
GHI	64		709		302		W/m^2
Wind speed	10.28	-	2.06	-	1.54	-	m/s
Air Temperature	12.82	-	20.84	-	21.80	-	$^{\circ}C$
FPV Output	15.62	15.62	171.50	171.50	73.69	73.69	W
Hydrogen Output	318.2	318.2	349.4	349.4	171.4	171.4	$tons$
RO Consumption	0.98	0.98	10.77	10.77	4.63	4.63	MW
Compressor Consumption	0.028	0.028	0.25	0.25	0.11	0.11	GW

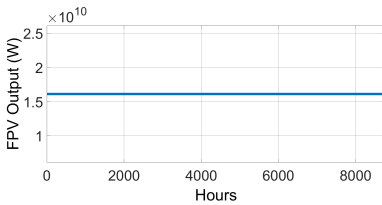
through the year, the FPV output is zero. In the same direction, by setting constant irradiance and trying maximum and medium values, the FPV output changes accordingly.



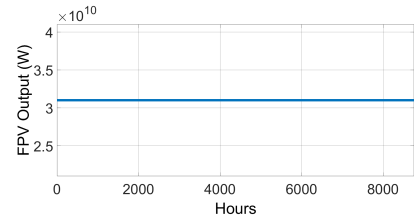
(a) Real Irradiance Data



(b) Zero Irradiance



(c) Medium Irradiance



(d) Maximum Irradiance

Figure A.1: FPV Power Output depending on the different irradiance levels

Furthermore, the hydrogen output should be proportionate to the FPV power output (for the configurations which do not use batteries) and therefore, to the irradiance of the selected location, limited by the capacity of the electrolyzer. In figure A.2, the hydrogen output for different irradiance levels is depicted, considering once again constant air temperature and wind speed values.

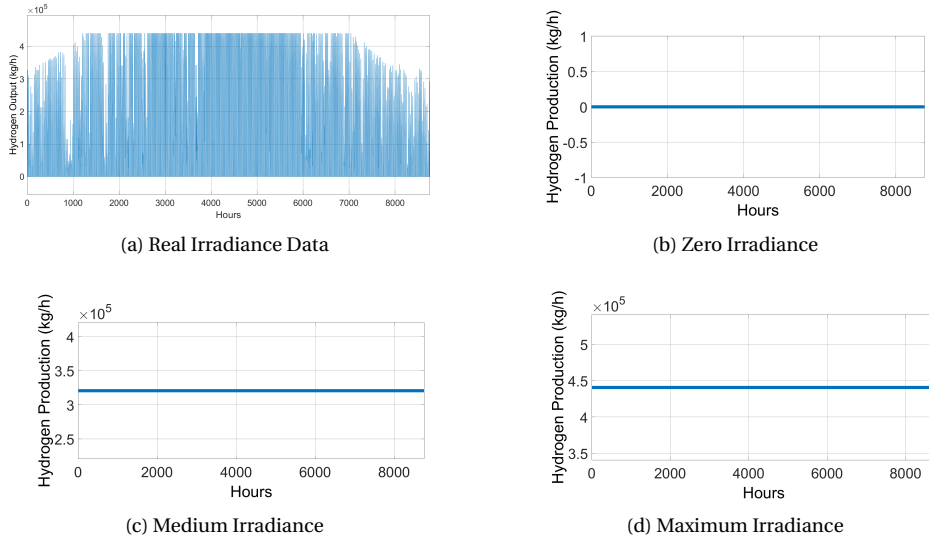


Figure A.2: Hydrogen Output for the configurations without batteries depending on the different irradiance levels.

From noticing figures A.1, A.2 it can be concluded that the model that calculates the FPV system power output and the hydrogen output operates as it was designed to, since the shape of the hydrogen output graphs are proportionate to the FPV system power output graphs which, in turn, are proportionate to the irradiance graphs.

The battery model is playing a crucial role in the final system selection and therefore it also needs to be verified. The results of the verification are presented in table A.2.

Table A.2: Verification of the battery model

Value	Model 1	Paper 1	Model 2	Paper 2	
PV Power	7500	-	0	-	W
Load	0	-	7500	-	W
Power to/from Battery	7600	7600	7895	7895	W
State of Charge	91.12	91.12	10.92	10.92	%

To do so, two set of input data were put in the Simulink model, one for charging and

A

one for discharging. The simulations run for 1 hour and the battery capacity is considered to be 10 kWh. The first set of values correspond to 7.5 kW for PV power, 0 W for load and the starting level of charge of the battery is 20%. Taking into account the charging efficiency (95%), the final charging level of battery is expected to be slightly below 100%. For the second set of values, 0 W is considered for the PV power and 7.5 kW for the load, while the starting level of charge of the battery is 95%. Therefore, the final state of charge after 1 hour is expected to be slightly higher than 5%. All the calculations were performed both in Simulink and on paper for the verification process.

B

APPENDIX

B.1. MODEL RESULTS

In total, four different system configurations were modelled and simulations were run for them. From the simulations, graphs were plotted to give insights on how the systems operate.

B.1.1. CONFIGURATIONS WITHOUT BATTERIES

In this system configurations, the power produced by the OFPV system is directly fed into the electrolyzer. To ensure optimal energy usage, power electronics are included. More specifically, DC-DC converters and maximum power point trackers (MPPT) are included in the system, as already explained in chapter 4. For this configurations, FPV system output is the only power source in the system. Therefore, all the energy generated power by the FPV system is used to produce hydrogen, including the energy provided for the the other facilities, such as the reverse osmosis plant, the compressor and the control systems, buffered by a small amount of batteries. The hydrogen production in the system is limited by the electrolyzer minimum and maximum capacity. If the output of the FPV system is higher than the electrolyzer rated capacity, or lower than the minimum capacity, then the extra power cannot be used for hydrogen production and is dumped.

ALKALINE ELECTROLYZER WITHOUT THE USE OF BATTERIES

In this system, the capacity of the OFPV system is calculated to be 32.6 GW. The output power of the FPV system (vertical axis) depending on the hours of the year, starting from January, is depicted in figure B.1. As can be seen in the figure, during the summer hours, the power output is the highest. The opposite can be seen about the winter hours, where the irradiance is significantly lower.

All the power produced by the FPV system is fed into the electrolyzer and the other facilities, after passing through the DC-DC converters. The rated power of the FPV system is calculated to be 22 GW. The load of the electrolyzer is restricted by the two operating limits of the electrolyzers. The upper limit is the rated capacity of the electrolyzer

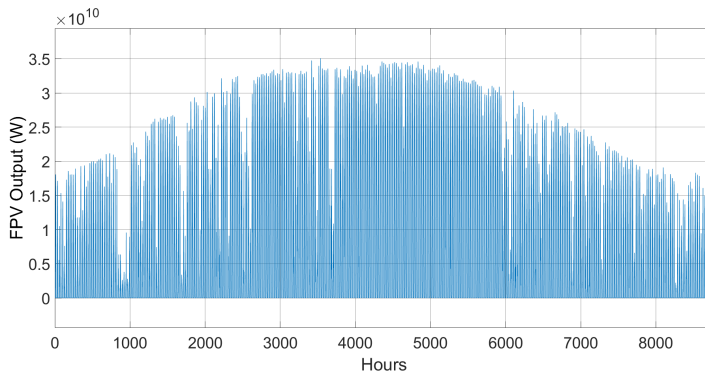


Figure B.1: FPV system power output in the alkaline system configuration with no battery addition

(22 GW) and the lower limit is the minimum power load of a single stack, which is 10% for alkaline electrolyzers. Considering that a single stack has a rated capacity of 5 MW, for OFPV power output less than 500 kW, the electrolyzer is shut down. The load of the electrolyzer is depicted in figure B.2:

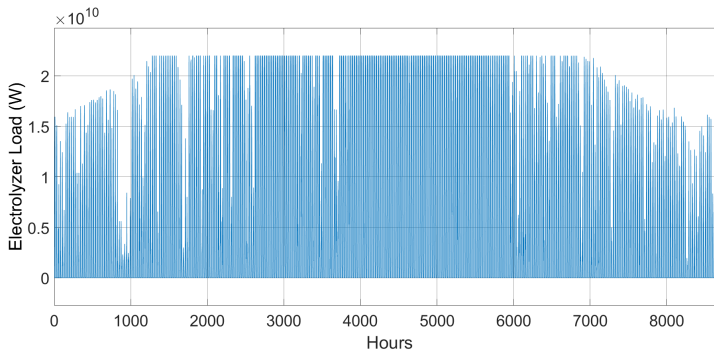


Figure B.2: Electrolyzer load in the alkaline system configuration with no battery addition

In general, as explained in chapter 4, sizing of the system is based on matching the FPV power output with the electrolyzer input. However, by varying the PV and electrolyzer capacity, it was found that it might be more cost-effective to size the PV system higher than the electrolyzer, and therefore, dump some power. All the power higher than the maximum and lower than the minimum load of the electrolyzer is wasted. Overall, this amount of energy represents the 6.3% of the total energy produced by the FPV system. Increasing the size of the electrolyzer to avoid wasting energy, leads to an oversized system, with increased LCOH of about 7% and therefore, it is preferred to waste this amount of energy.

The hydrogen production, depicted in B.3, is directly proportional to the electrolyzer load. The total annual hydrogen production for this configuration, was calculated to be 1.03 millions tons. The capacity factor of the electrolyzer is calculated by dividing

the actual hydrogen production through the year, with the hydrogen production, if the electrolyzer run at the rated capacity. For this case, the capacity factor is 24.6%. Another interesting number is the hours in which the electrolyzer operates at full load through the year. For this configuration, the electrolyzer runs at its rated capacity for 822 hours through the year.

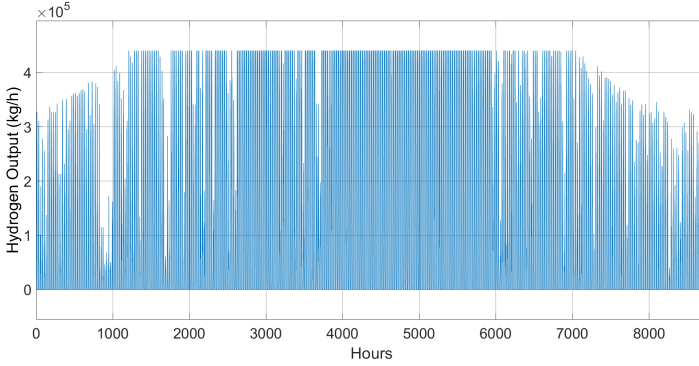


Figure B.3: Hydrogen Production in the alkaline system configuration with no battery addition

In table B.1, the information about the alkaline configuration without batteries are presented.

Table B.1: Results of the simulation for the configuration based on alkaline electrolysis without batteries

PV system [GW]	Electrolyzer [GW]	Batteries [GWh]	Capacity Factor [%]	Hours Operating at Full Load	LCOH [€/kg]
32.6	22	4.4	24.6	822	1.5

PEM ELECETROLYZER WITHOUT THE USE OF BATTERIES

In this system, the rated capacity of the PV system is 37.3 GW. The output power of the FPV system is depicted in figure B.4.

Like in the alkaline case, the FPV power output has the shape expected, including peaks during the summer hours and smaller peaks during the winter hours. Once again here, the FPV power output is depicted before losses are taken into account. The load of the electrolyzer is depicted in figure B.5. The maximum electrolyzer capacity is 22 GW. For the lower case, PEM electrolyzer support flexible operation better than alkaline and the minimum load can reach even 0%. All the generated power that is higher than the maximum capacity and lower than the minimum capacity is wasted. Overall, this amount of energy represents the 9.4% of the total energy produced by the FPV system. This amount is higher than the respective alkaline case, due to the higher capacity of the FPV system.

For this system, the capacity factor is 25.9%, a number almost equal to the alkaline case, which is reasonable since the same electrolyzer capacity was used. The hours in

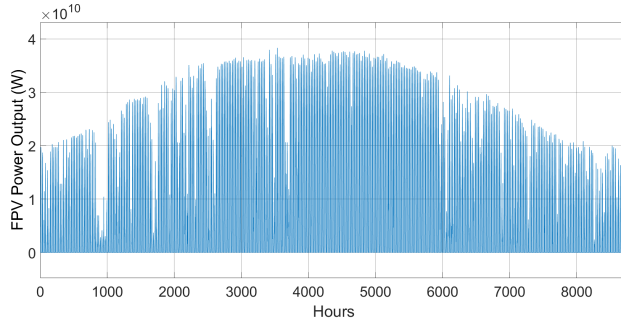


Figure B.4: FPV System Power Output in the PEM system configuration with no battery addition

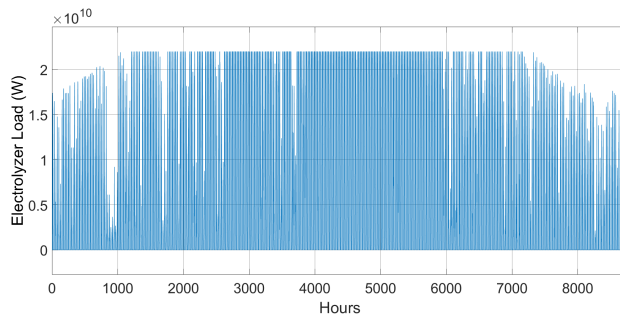


Figure B.5: Electrolyzer load in the PEM system configuration with no battery addition

which the electrolyzer operates at full load are 1088, which is higher than the alkaline case due to the higher FPV power output. The total annual hydrogen production for this configuration, was calculated to be 1.02 millions tons. The hydrogen production per hour is depicted in figure B.6:

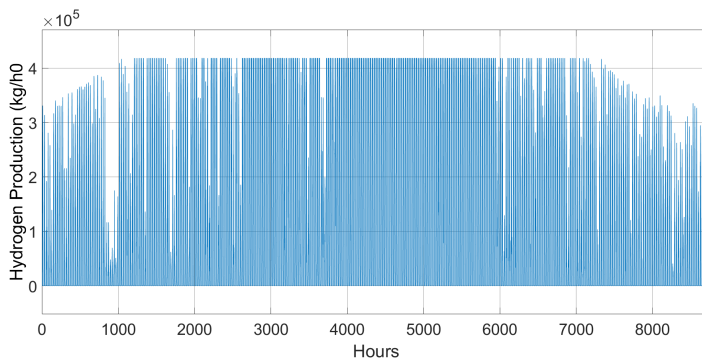


Figure B.6: Hydrogen Production in the PEM system configuration with no battery addition

In table B.2, the information about the PEM configuration without batteries are presented. The LCOH for this case is higher than the alkaline one, due to the higher costs of the PEM electrolyzers compared to alkaline, and the extra PV power needed.

Table B.2: Results of the simulation for the configuration based on PEM electrolysis without batteries

PV system [GW]	Electrolyzer [GW]	Batteries [GWh]	Capacity Factor [%]	Hours Operating at Full Load	LCOH [€/kg]
37.3	22	4.4	25.9	1088	1.8



B.1.2. CONFIGURATIONS WITH BATTERIES

In chapter 4, the control strategy of the battery configurations was presented. This strategy modifies the load setting of the electrolyzer. Electrolyzers are preferred to operate with a constant power supply, which does not mean that they cannot operate otherwise. To be able to provide this constant power to the electrolyzer, batteries are used. Batteries also help utilize the generated energy in a more optimal way. It should be mentioned again at this point, that battery addition to the system intends to keep it open during the night, stabilize the electrolyzer input load, and in general, ensure a better and smoother operation of the electrolyzer.

ALKALINE ELECTROLYZER WITH THE USE OF BATTERIES

Alkaline electrolyzers, in order to operate throughout all the year, need to operate at least at 10% of the rated power. Therefore, a significant amount of batteries is expected to be used. The rated capacity of the FPV system is calculated to be 33.5 GW. It is higher than the one in the no battery configuration, and this is due to the lower electrolyzer capacity and the battery effect. The output power of the FPV system is depicted in figure B.7.

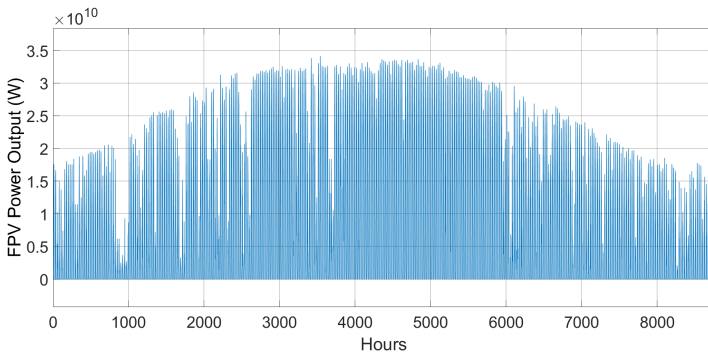


Figure B.7: FPV System Power Output in the alkaline system configuration with batteries

The electrolyzer capacity, in this system, is calculated to be 19 GW, which is lower than the no battery configuration due to the use of batteries. As can be seen in figure B.8, the electrolyzer input power is split in five load levels, with the lowest level to be 10% of the rated capacity. The target is that by using a battery system, the alkaline electrolyzer can operate during all the hours of the year. The generated power is distributed to the electrolyzer and the battery, following the algorithm specified in chapter 4, that defines the power control strategy. By keeping the electrolyzer operating at 10% of its capacity, the electrolyzer does not have to turn off even at the night hours.

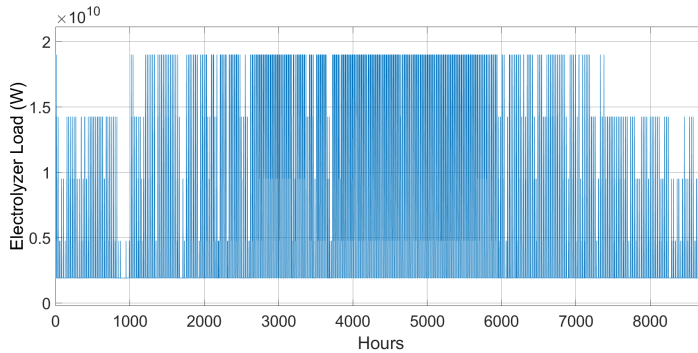


Figure B.8: Electrolyzer load in the alkaline system configuration with batteries

Similar to the electrolyzer, the battery has also operating boundaries. The lower limit for lithium ion batteries is 5% and the higher is 95%. After crossing these boundaries, the battery stops charging or discharging. The battery state of charge can be seen in figure B.9. During the winter hours, the battery is not optimally used, due to the low irradiance levels, that do not allow excess power to be generated by the PV modules.

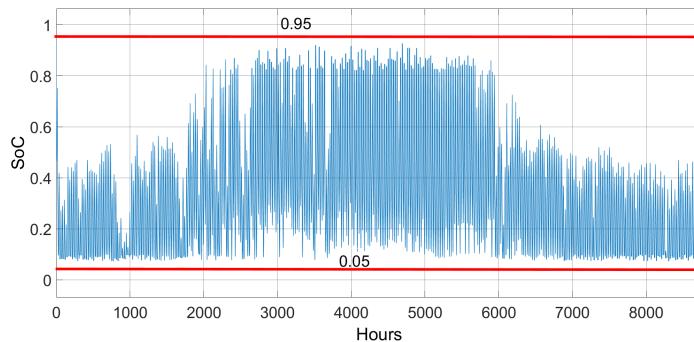


Figure B.9: Battery state of charge (SoC) in the alkaline system configuration with batteries

On the contrary, during summer hours, the battery cannot store all the generated energy and the system is forced to dump the excess energy. The battery capacity needed is 52.65 GWh, a high number for a single system. It is a reasonable number since the system

is intending for large-scale, however, it is almost half of the current global lithium-ion battery production.

The hydrogen production is depicted in figure B.10. For this case, the capacity factor is 28.5%, which is higher than the system without the use of batteries and that is totally justified due to the better energy usage with the use of batteries. The full load hours here, are increased from the no battery configuration and equal to 1204, due to the control strategy which depending on the charging limits of the battery, may allow the electrolyzer to operate at its maximum load.

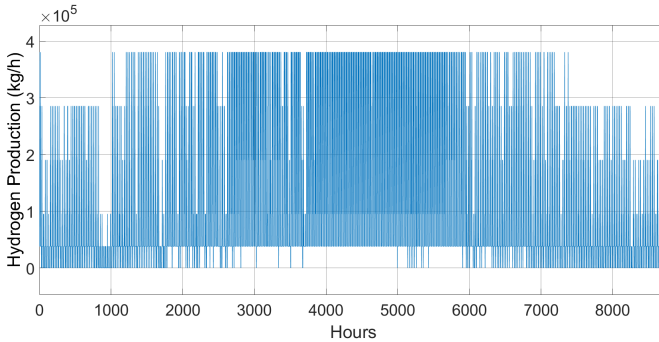


Figure B.10: Hydrogen Production in the alkaline system configuration with batteries

As can be seen in the figure, there are times of energy surplus and deficit in the system. The former one, happens when the electrolyzer already operates at maximum capacity and batteries are fully charged. Opposite to that, energy deficit takes place in the system when the FPV power is lower than the minimum operating capacity of the electrolyzer system, and the energy in the battery system is not sufficient to ensure the operation of the electrolyzer. The reason for this energy mismatch is the significant difference in the irradiance levels between the seasons of the year, summer and winter. Including more PV modules and batteries can provide the solution, but it will lead to an oversized system, with LCOH reaching 2.9 (€/kg). In general, based on equation 4.6, if running the electrolyzer at rated capacity for all the hours of the year, 5.41 GW of electrolysis are needed. However, this is not possible in practice, since large amounts of PV and batteries are needed. The hydrogen production of this system, is 1.03 million tons per year. In total, 3.1 % of the energy is dumped in this configuration, decreased from the previous ones, because of the battery use. In table B.3, the information about the alkaline configuration with batteries are presented :

Table B.3: Results of the simulation for the configuration based on alkaline electrolysis with batteries

PV system [GW]	Electrolyzer [GW]	Batteries [GWh]	Capacity Factor [%]	Full Load Hours	LCOH [€/kg]
33.5	19	52.7	28.5	1204	2.0

PEM ELECTROLYZER WITH THE USE OF BATTERIES

The capacity of the FPV system is 36.9 GW. The output power of the FPV system is depicted in figure B.11:

B

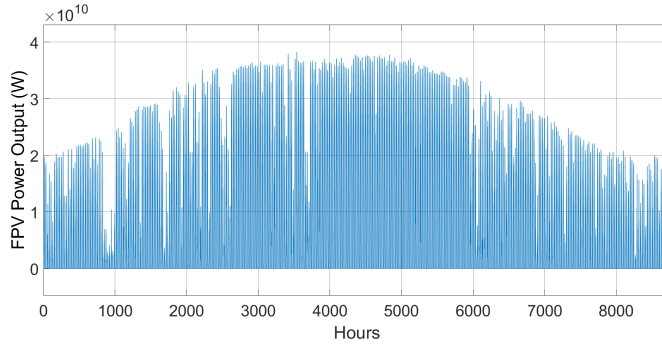


Figure B.11: FPV System Power Output in the alkaline system configuration with batteries

Once again, for the configurations including batteries, different levels are set for the electrolyzer operation. The difference with the alkaline case, is the lower possible limit, which in the PEM case is considered 1 %, as can be seen in figure B.12. The rated capacity of the electrolyzer facility is 22 GW. In this system, 7.4% of the power is dumped.

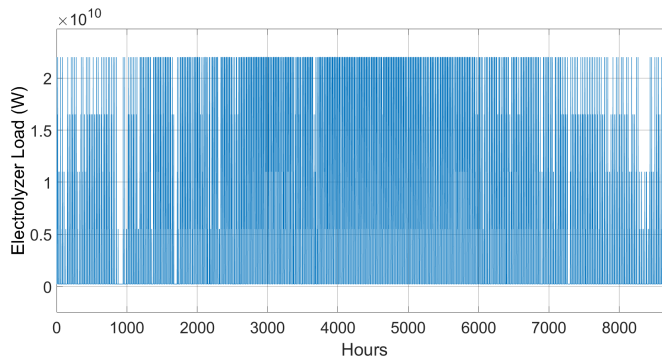


Figure B.12: Electrolyzer load in the PEM system configuration with batteries

In this configuration, much less battery power is needed, due to the different level of minimum operation of the electrolyzer. The battery capacity needed is 44 Gwh. The battery state of charge can be seen in figure B.13:

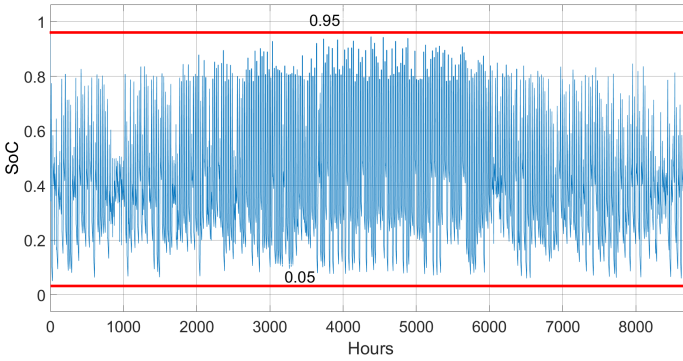


Figure B.13: Battery state of charge (SoC) in the alkaline system configuration with batteries

In this configuration, as can be noticed in in figure B.14, there are no moments of deficit and the system operated during all the year. For this case, the capacity factor is 25.9%, while the full load hours here, are increased from the no battery configuration and equal to 1373, due to the control strategy which depending on the charging limits of the battery, may allow the electrolyzer to operate at its maximum load.

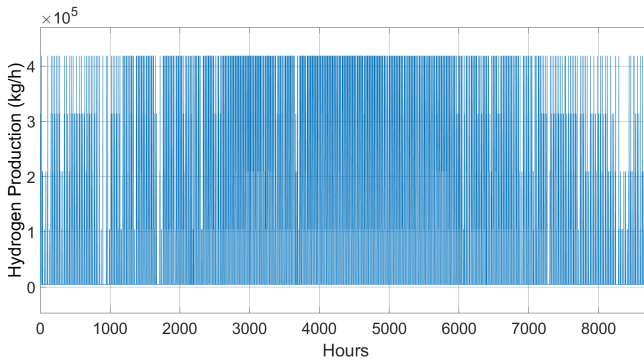


Figure B.14: Hydrogen Production in the alkaline system configuration with batteries

In table B.4, the information about the PEM configuration with batteries are presented. The LCOH for this case is higher than the PEM configuration without the batteries, due to the high costs of the battery systems.

Table B.4: Results of the simulation for the configuration based on PEM electrolysis with batteries

PV system [GW]	Electrolyzer [GW]	Batteries [GWh]	Capacity Factor [%]	Full Load Hours	LCOH [€/kg]
36.9	22	40.2	25.9	1373	2.2